



Calhoun: The NPS Institutional Archive
DSpace Repository

Theses and Dissertations

1. Thesis and Dissertation Collection, all items

1975

Improvements to simple radial equilibrium preliminary turbine design.

Larson, William Douglas

Massachusetts Institute of Technology

<http://hdl.handle.net/10945/20899>

Downloaded from NPS Archive: Calhoun



<http://www.nps.edu/library>

Calhoun is the Naval Postgraduate School's public access digital repository for research materials and institutional publications created by the NPS community. Calhoun is named for Professor of Mathematics Guy K. Calhoun, NPS's first appointed -- and published -- scholarly author.

Dudley Knox Library / Naval Postgraduate School
411 Dyer Road / 1 University Circle
Monterey, California USA 93943

IMPROVEMENTS TO SIMPLE RADIAL EQUILIBRIUM
PRELIMINARY TURBINE DESIGN

William Douglas Larson

2025 RELEASE UNDER E.O. 14176
NAVAL POSTGRADUATE SCHOOL
MONTEREY, CALIFORNIA 93940

IMPROVEMENTS TO SIMPLE RADIAL EQUILIBRIUM

PRELIMINARY TURBINE DESIGN

by

WILLIAM DOUGLAS LARSON

B.S., University of Chicago
(1967)

M.S., University of Minnesota
(1969)

Submitted in Partial Fulfillment
of the Requirements for the
Degrees of

NAVAL ARCHITECT

and

MASTER OF SCIENCE IN MECHANICAL ENGINEERING

at the

MASSACHUSETTS INSTITUTE OF TECHNOLOGY

May, 1975

IMPROVEMENTS TO SIMPLE RADIAL EQUILIBRIUM PRELIMINARY TURBINE DESIGN

by

William D. Larson

Submitted to the Department of Ocean Engineering on
May 9, 1975, in partial fulfillment of the requirements
for the degrees of Naval Architect and Master of Science
in Mechanical Engineering.

ABSTRACT

Although simple radial equilibrium turbine design has long been a useful design method for axial flow gas turbine blading, more demanding requirements for high performance machinery make such an approximation less justified. More exact analytical methods do exist, but require many times more effort, even if a computer is utilized.

A relatively simple model for improving a simple radial equilibrium preliminary design is proposed in this thesis. The axial velocity distribution, determined from the input SRE design, is modified to take into account the results of flow studies in flared annuli and of actuator disk theory. Using the corrected axial velocity distribution, new velocity triangles can be calculated.

A FORTRAN IV computer program to implement the proposed model was written and is presented. Its potential is demonstrated by application to three example simple radial equilibrium designs. The results show practical differences exist between a simple radial equilibrium design and the design corrected by the proposed method.

Thesis Supervisor: A. Douglas Carmichael
Title: Professor of Power Engineering

Thesis Reader: David Gordon Wilson
Title: Professor of Mechanical Engineering

ACKNOWLEDGEMENT

The author extends his appreciation to Professor A. Douglas Carmichael, under whose guidance this work was accomplished.

An expression of gratitude is also owed my wife, Dottie, for her constant encouragement and understanding through the highs and lows of this project.

TABLE OF CONTENTS

	<u>PAGE</u>
TITLE PAGE	1
ABSTRACT	2
ACKNOWLEDGEMENT	3
TABLE OF CONTENTS	4
LIST OF FIGURES AND TABLES	7
NOTATION	9
1. INTRODUCTION	
1.1 General	11
1.2 Axial Flow Turbines	11
1.3 Aerodynamic Design of Axial Flow Turbines	12
1.3.1 General	12
1.3.2 Flow Solutions	13
1.3.3 Two-Dimensional Flow	14
1.3.4 Three-Dimensional Flow	14
1.4 Approaches to Three-Dimensional Design	14
1.4.1 Radial Equilibrium	14
1.4.2 Simple Radial Equilibrium	15
1.4.3 Actuator Disk Theory	15
1.5 Fluid Flow in Flared Annuli	16
1.6 Summary	16
2. BACKGROUND	
2.1 Fluid Mechanics	18
2.2 Thermodynamics	19
2.2.1 Work	19
2.2.2 Gas Laws	20
2.2.3 The Second Law	21
2.3 Compressible Flow Relations	21

2.4	Simple Radial Equilibrium	23
2.4.1	General	23
2.4.2	Simple Radial Equilibrium Equation .	24
2.4.3	Solutions to the Simple Radial Equilibrium Equation	27
2.5	Actuator Disk Theory	30
2.5.1	General	30
2.5.2	Approximate Solution	32
2.6	Flow in Flared Annuli	33
2.6.1	General	33
2.6.2	Experiments Representing Fluid Flow in Flared Turbines	34
2.7	Axial Turbine Flow Geometry	37
2.7.1	Velocity Triangles	37
2.7.2	Annulus Area	39
3.	MODEL DESCRIPTION AND IMPLEMENTATION	
3.1	General	41
3.2	Model Description	41
3.2.1	The Input Design	42
3.2.2	Calculating the Streamlines	44
3.2.3	Velocity Triangle Data	46
3.3	Computer Implementation of the Model . . .	46
3.3.1	General	46
3.3.2	Procedure Steps	47
3.3.3	Overall Program	49
3.3.4	Reading and Processing Input Data . .	49
3.3.5	Calculating a Streamline Location . .	52
3.3.6	Calculating V_x and V_θ (Simple Radial Equilibrium)	56
3.3.7	Generating a Feasible Streamline Set at a Plane	56
3.3.8	Adjusting $VXR(I)$	57
3.3.9	Correcting Axial Velocity for Flare .	59
3.3.10	Correcting Axial Velocity for Actuator Disk Effects	60
3.3.11	Testing for Overall Streamline Convergence	60
3.3.12	Velocity Triangle Calculations . . .	61
3.3.13	Iteration Test Values	62

3.4	Convergence Checks	64
3.5	Program Verification	64
4.	RESULTS	
4.1	General	67
4.2	Free Vortex Design	67
4.3	Constant Reaction Design	68
4.4	Free Vortex, High Mach Number Design	69
5.	CONCLUSIONS	
5.1	General	87
5.2	Improving the Model	88
5.3	Applications	88
	REFERENCES	89
	APPENDICES	
A.	Variable List	90
B.	Program Listing	95
C.	Specific Instructions for Use of the Program112
D.	Integration of the Simple Radial Equilibrium Equation123
E.	Actuator Disk Superposition126
F.	Calculation of the Flare Geometry Factors	.130

LIST OF FIGURES AND TABLES

<u>Figure</u>	<u>Title</u>	<u>Page</u>
2-1	Derivation of Simple Radial Equilibrium Equation	26
2-2	Radial Flow Models	31
2-3	Flare Angle Definition	35
2-4	Flare Geometry	35
2-5	Axial Velocity Vs. Flare Angle	36
2-6	Single Stage Axial Turbine Velocity Triangles	38
2-7	Annulus Area Geometry	40
3-1	Model Geometry and Input Requirements . . .	43
3-2	Overall Computer Program: MAIN	50
3-3	Subprogram RNEXT	53
3-4	Subroutine STREAM	55
3-5	MAIN: Iteration for Streamlines	58
3-6	MAIN: Calculation of Velocity Triangles . .	63
3-7	Loop Divergence Testing	65
4-1	Example 1: Input Data	70
4-2	Example 1: Geometry	71
4-3	Example 1: Results	72
4-4	Example 1: Results	73
4-5	Example 1: Results	74
4-6	Example 1: Results	75
4-7	Example 2: Input Data	76
4-8	Example 2: Results	77
4-9	Example 2: Results	78

4-10	Example 2: Results	79
4-11	Example 2: Results	80
4-12	Example 3: Input Data	81
4-13	Example 3: Geometry	82
4-14	Example 3: Results	83
4-15	Example 3: Results	84
4-16	Example 3: Results	85
4-17	Example 3: Results	86
C-1	Sample Diagnostic Data	122
E-1	Actuator Disk Superposition	128
F-1	Derivation of Flare Parameters	131

NOTATION

A	flow area, ft^2
a	coefficient in equations 2.24, 2.25, 2.27, and 2.28
A_{ann}	annulus area, ft^2
b	coefficient in equations 2.24, 2.25, 2.27, and 2.28
c_p	specific heat at constant pressure, $\text{BTU/lbm}/^\circ\text{R}$
c_v	specific heat at constant volume, $\text{BTU/lbm}/^\circ\text{R}$
g_o	$32.2 \text{ ft lbm/lbf/sec}^2$
h	specific enthalpy, BTU/lbm ; actuator disk height, ft
J	778 ft lbf/BTU
M	Mach number
\dot{m}	mass flow rate, lbm/sec
N	turbine rpm, revolutions per minute
P	pressure, lbf/ft^2
\dot{Q}	rate of heat transfer to fluid, BTU/sec
r	radial distance from machine axis, ft
\bar{R}	specific gas constant, $\text{ft lbf/lbm}/^\circ\text{R}$
s	specific entropy, $\text{BTU/lbm}/^\circ\text{R}$
T	temperature, $^\circ\text{R}$
u	blade velocity, ft/sec
V	fluid velocity, ft/sec
\dot{W}	rate of output shaft work, BTU/sec
W	relative velocity, ft/sec
x	axial distance from an actuator disk, ft

α	absolute angle measured from axis, degrees
$\Delta\alpha$	stator turning angle, degrees
β	relative angle measured from axis, degrees
$\Delta\beta$	rotor turning angle, degrees
γ	specific heat ratio
ρ	density, lbm/ft ³
ϕ	flare angle, degrees
ω	angular velocity, radians/sec

Subscripts

h	hub condition
i	reference condition
o	total (stagnation) condition
r	radial component
rel	relative
t	tip condition
x	axial component
θ	tangential component
1	rotor inlet; plane one condition
2	rotor outlet; plane two condition
3	plane three condition
$+\infty$	condition far downstream
$-\infty$	condition far upstream

NOTE: Notation not appearing here may be computer program variables listed in Appendix A.

1. INTRODUCTION

1.1 General

Energy is a topic of increased interest in current times. Searches for new sources of energy and new means of converting energy into useful forms have been undertaken, along with efforts to conserve the resources available. While exploiting solar energy, tapping geothermal power, and drilling for oil off-shore receive much public interest, progress in improving existing conventional forms of energy transfer and conversion must also be made. The great importance of energy utilization has made it worthwhile for designers of energy related systems to pay even more attention to achieving the best possible performance. Improving the efficiencies of the various hardware components which carry out the heat transfers and energy conversion functions of the thermal cycle is one desirable goal. To accomplish this, it is useful to make design methods more accurate and more easily applied to real problems.

1.2 Axial Flow Turbines

This thesis deals with one commonly used component for converting energy into useful work--the axial flow turbine. Turbines convert the kinetic energy which has been provided the working fluid into mechanical work

performed upon a rotating shaft. Axial flow turbines are so named because the flow of the working fluid through the machine is predominantly in a direction parallel to the machine's axis of rotation. Such turbines can operate with a variety of working fluids, and in either open or closed thermal cycles. The most common configurations are as a steam turbine in the Rankine Cycle (a closed cycle) or as a gas turbine in the Brayton Cycle (an open or closed cycle). Historically, the steam turbine found earlier application than the gas turbine, which recently has gained in importance. The development of the gas turbine depended upon advances in high temperature material properties and was also closely tied to the successful operation of axial compressors.

1.3 Aerodynamic Design of Axial Flow Turbines

1.3.1 General

One aspect of the design, which proceeds similarly for axial turbines of all kinds, is the aerodynamic design of the turbine blading. The efficiency of the turbine depends upon the smooth transfer of kinetic energy from the fluid flow, with as little energy wasted as possible. The shapes and angles of the turbine blading must be appropriate to the pattern of the flow. The aerodynamic design of the turbine determines what these flows and shapes should be.

In general, the aerodynamic designer of an axial turbine follows the steps listed below:

(1) for an assumed operating point and efficiency, carry out the thermodynamic analysis of the thermal cycle to determine the mass flow, and inlet and outlet states for the turbine;

(2) postulate a working fluid flow which satisfies the laws of motion and produces the required work;

(3) design the shape of the turbine blading appropriately;

(4) calculate the efficiency and evaluate the design;

(5) repeat all of the above steps as necessary.

1.3.2 Flow Solutions

As is true of most design efforts, there are many levels of sophistication and detail which the designer may seek, depending upon the stage of the design and/or the cost and criticality of the product. In the aerodynamic design of a turbine, the designer must decide which level is best in each case. For, although the equations of motion and continuity for a fluid are readily written, they cannot be solved in practice unless simplifying assumptions are made. Fortunately, such simplified forms have proved adequate in many applications.

1.3.3 Two-Dimensional Flow

If the hub-tip ratio of a turbine is nearly 1.0, no large radial component of fluid velocity is expected, and flow conditions will be approximately the same from root to tip. The flow can then be analyzed in two dimensions. This results in blades of constant cross-section, which have been extensively studied experimentally in the form of cascades.

1.3.4 Three-Dimensional Flow

In some cases the designer faces requirements on blade tip speed, pressure ratio, and mass flow which could result in low hub-tip ratios (i.e., relatively long blades) and considerable turbine flare. These conditions reduce the accuracy of simple two-dimensional design methods and force the consideration of three-dimensional flow. The general solution is impractical, but simplified methods have been developed and used with success. Several of these approaches are mentioned below.

1.4 Approaches to Three-Dimensional Design

The first assumption made in virtually all cases is to assume axial symmetry. The number of blades is sufficiently large that circumferential conditions at a station can be represented by average values.¹

1.4.1 Radial Equilibrium

Assuming axisymmetric flow, the differential equation of motion in the radial direction for the fluid

can be put in a form (see paragraph 2.4.1) which may be numerically integrated by a computer. The procedure involves complicated iterations, however, and elaborate measures must be taken to ensure the proper convergence of the streamline locations. Carmichael has discussed the procedure and presented block diagrams of possible computer programs.¹ This method allows for fluid velocities in the radial direction which result from imbalances in the static pressure and centrifugal acceleration forces on the fluid, but its complexity is formidable.

1.4.2 Simple Radial Equilibrium

If the radial components of the fluid velocity are neglected, the so-called streamline curvature term in the differential equation drops out. The differential equation of motion in the radial direction can then be written involving only the axial and tangential velocities. This can be easily integrated for axial velocity when given a reasonable distribution for the tangential velocity (see paragraph 2.4.3). Simple pairs of functions for axial and tangential velocity, so determined, have been widely used in three-dimensional design.

1.4.3 Actuator Disk Theory

Simple radial equilibrium analysis depended upon the radial fluid velocity being zero before and after each blade row. In most cases, changes in the radial distribution of density result in radial shifts in the

streamlines. Therefore, a non-zero radial velocity component must exist.

An alternative to the simple radial equilibrium analysis is the actuator disk formulation. Each blade row is replaced by a narrow "actuator disk" which provides the appropriate sudden change in fluid tangential velocity. This device permits an approximate solution to the equations of motion, allowing finite radial velocities, but still is restricted to annular flow between walls parallel to the machine axis. (See paragraph 2.5)

1.5 Fluid Flow in Flared Annuli

A frequent design practice is to keep the axial velocity approximately constant throughout the machine, compensating for changes in fluid density by increasing the annulus area. This area change results in "flare"; that is, the hub and shroud surfaces are not parallel to the machine axis, but are sloped.

This flare could be expected to cause a general change in the axial velocity distribution within the annulus, with significant radial velocity components appearing near the walls. Carmichael and Pai² have suggested a relation which can be used to calculate the change in axial velocity in flared annuli.

1.6 Summary

The preceding discussion was intended to demonstrate a need for a relatively simple method to predict the

fluid flow distribution in the presence of flare, improving upon the accuracy of the simple radial equilibrium model. Such a method would hopefully be useable in the preliminary design phase with little increased effort, as compared to the more complicated streamline curvature approaches.

A method is proposed in this thesis for "correcting" a preliminary simple radial equilibrium turbine design for flare and streamline curvature effects. This is accomplished by modifying the axial velocity radial variation, as determined from the simple radial equilibrium equations. A correction for turbine flare is applied using the findings of Pai; next, the axial velocity is further modified at the blade leading and trailing edges by the approximate solutions to the actuator disk analysis. As the computations are still iterative in nature, they are very suitable for computerization.

A computer program to modify a simple radial equilibrium turbine design, according to the model described above, is presented in this thesis. While not theoretically deep-seated, it is hoped the methodology may be helpful in some turbine design applications.

2. BACKGROUND

The purpose of this chapter is to provide the background for the methodology employed in the computer model to be discussed in Chapter 3. The emphasis is placed on those assumptions and relations which directly apply to the program model, although some additional development is included for perspective and to point to possible areas of application and further work.

2.1 Fluid Mechanics

Axial turbine flow is frequently modeled as incompressible, at least in the radial direction, so that the equations of motion for an incompressible fluid apply. It is also known that viscous effects can usually be neglected outside the boundary layer.¹ In cylindrical coordinates, the equations of motion for an ideal, incompressible fluid can be written as³

$$V_r \frac{\partial V_r}{\partial r} + \frac{V_\theta}{r} \frac{\partial V_r}{\partial \theta} + V_x \frac{\partial V_r}{\partial x} - \frac{V_\theta^2}{r} = - \frac{g_O}{\rho} \frac{\partial P}{\partial r} \quad (2.1)$$

$$V_r \frac{\partial V_\theta}{\partial r} + \frac{V_\theta}{r} \frac{\partial V_\theta}{\partial \theta} + V_x \frac{\partial V_\theta}{\partial x} + \frac{V_r V_\theta}{r} = - \frac{g_O}{\rho r} \frac{\partial P}{\partial \theta} \quad (2.2)$$

$$V_r \frac{\partial V_x}{\partial r} + \frac{V_\theta}{r} \frac{\partial V_x}{\partial \theta} + V_x \frac{\partial V_x}{\partial x} = - \frac{g_O}{\rho} \frac{\partial P}{\partial x} , \quad (2.3)$$

where V_r , V_θ , and V_x refer to components of fluid velocity in the radial, tangential, and axial directions, respectively. P is the static pressure. The continuity equation is

$$\frac{\partial V_r}{\partial r} + \frac{V_r}{r} + \frac{1}{r} \frac{\partial V_\theta}{\partial \theta} + \frac{\partial V_x}{\partial x} = 0. \quad (2.4)$$

2.2 Thermodynamics

2.2.1 Work

From the first law of thermodynamics, the steady flow energy equation, describing the change in state of a fluid system in flowing through a control volume, can be written as⁴

$$\dot{Q} - \dot{W} = \dot{m} \left[\left(h + \frac{V^2}{2g_o J} \right)_{out} - \left(h + \frac{V^2}{2g_o J} \right)_{in} \right], \quad (2.5)$$

where potential terms have been ignored. \dot{Q} is the rate of heat transfer to the fluid, \dot{W} is the rate of output shaft work, \dot{m} is the mass flow, V is the fluid velocity, and h is the enthalpy. A useful definition is to make stagnation enthalpy, h_o ,

$$h_o \equiv h + \frac{V^2}{2g_o J} \quad (2.6)$$

Using equation (2.6), and assuming that the heat transfer, \dot{Q} , from an axial turbine is small (compared to \dot{W}), equation (2.5) becomes

$$-\dot{W} = (h_{o2} - h_{o1}) \cdot \dot{m}, \quad (2.7)$$

where the 2 and 1 refer to the outlet and inlet states respectively.

Following reference 1, the rate of output shaft work, \dot{W} , is also equal to the product of the angular velocity, ω , of the blades and the torque caused by the moments of the external reaction forces. The torque is given by the change in angular momentum of the fluid, or

$$\text{Torque} = \dot{m}(r_2 V_{\theta 2} - r_1 V_{\theta 1}). \quad (2.8)$$

Since

$$\dot{W} = \text{Torque} \cdot \omega$$

and the blade velocity, u , is just ωr , then

$$\frac{\dot{W}}{\dot{m}} = \frac{u_2 V_{\theta 2} - u_1 V_{\theta 1}}{g_o J}. \quad (2.9)$$

In axial machines it is a good assumption to make $u_2 = u_1 = u$ for preliminary design.

2.2.2 Gas Laws

The equation of state for a perfect gas can be written

$$P = \rho \bar{R}T, \quad (2.10)$$

where \bar{R} is the specific gas constant. The following relations between the specific heats are the standard ones.

$$\gamma \equiv \frac{C_p}{C_v}$$

$$C_p - C_v = \bar{R}/J$$

$$C_p = \left(\frac{\gamma}{\gamma-1}\right) \frac{\bar{R}}{J}. \quad (2.11)$$

2.2.3 The Second Law

From the second law of thermodynamics, using Gibbs Equation and the perfect gas law, the specific entropy, s , can be written as^{1,5}

$$Tds = dh - \frac{1}{\rho J} dP. \quad (2.12)$$

2.3 Compressible Flow Relations

In all but very low speed turbomachines, in which velocity, pressure, and temperature changes are very small, the effects of compressibility of the working fluid become important. Consideration of three-dimensional compressible flow is extremely complex. Fortunately, the changes in fluid density are often not great in the

radial direction at a station, and need to be considered only in the axial flow direction.

The one-dimensional compressible flow relations for an ideal gas appear in many representations and are conveniently used. Horlock³ has a discussion of their derivation and summarizes the results. The following forms will be useful in discussion later. The meanings of the symbols can be found in the notation list. From equation (2.6), since, for a perfect gas, $h = c_p \cdot T$,

$$T_o = T + \frac{V^2}{2g_o J C_p}. \quad (2.13)$$

Using (2.11) and dividing by T_o , equation (2.13) can be rewritten as

$$\frac{T}{T_o} = 1 - \left(\frac{\gamma-1}{\gamma}\right) \frac{V^2}{2g_o \bar{R} T_o}. \quad (2.14)$$

The Mach number, M , is defined by

$$M \equiv \frac{V}{a} = \frac{V}{\sqrt{g_o \gamma \bar{R} T}}. \quad (2.15)$$

From equations (2.14) and (2.15),

$$\left(\frac{1}{M}\right)^2 = \frac{T_o g_o \gamma \bar{R}}{V^2} - \frac{\gamma-1}{2}. \quad (2.16)$$

The pressure-temperature relation for an isentropic process can be shown to apply in the compressible case, and gives

$$\frac{\rho}{\rho_0} = \left(\frac{T}{T_0}\right)^{\frac{1}{\gamma-1}}. \quad (2.17)$$

From continuity, the flow area, A , is

$$A = \frac{\dot{m}}{\rho V}, \quad (2.18)$$

which can be determined from equations (2.14) and (2.17) above.

2.4 Simple Radial Equilibrium

2.4.1 General

As indicated in the introduction, when the hub-tip ratio of a turbine stage is further and further from the value of 1.0 (i.e., relatively longer and longer blades), the two-dimensional flow design methods become less and less adequate. In some marginal cases, three-dimensional details of the design are ignored in favor of other considerations, for example, maintaining constant blade sections. But modern performance requirements make such practices less attractive. The general three-dimensional flow equations are difficult to solve, however, and simplifying assumptions are frequently made. The most general such assumption is to neglect any variation of

properties in the circumferential direction. In the axial direction, where fluid property changes may be large, the one-dimensional compressible flow relations are assumed to describe the flow. Finally, in the radial direction the equation of motion in a simplified form--termed the simple radial equilibrium (SRE) equation--is often applied. A discussion of the development and use of the simple radial equilibrium equation follows.

2.4.2 The Simple Radial Equilibrium Equation

Assuming axial symmetry, the equation of motion in the radial direction, equation (2.1), can be written as

$$V_r \frac{\partial V_r}{\partial r} + V_x \frac{\partial V_r}{\partial x} - \frac{V_\theta^2}{r} = - \frac{g_o}{\rho} \frac{\partial P}{\partial r}. \quad (2.19)$$

From the identity $\dot{V}^2 = V_r^2 + V_\theta^2 + V_x^2$ and by differentiating with respect to r , equation (2.6) becomes

$$\frac{\partial h}{\partial r} = \frac{\partial h_o}{\partial r} - \frac{1}{g_o J} [V_r \frac{\partial V_r}{\partial r} + V_\theta \frac{\partial V_\theta}{\partial r} + V_x \frac{\partial V_x}{\partial r}], \quad (2.20)$$

and equation (2.13) can be rewritten in the form

$$- \frac{1}{\rho J} \frac{\partial P}{\partial r} = T \frac{\partial s}{\partial r} - \frac{\partial h}{\partial r}. \quad (2.21)$$

Substitution of equations (2.20) and (2.21) into equation (2.19) gives

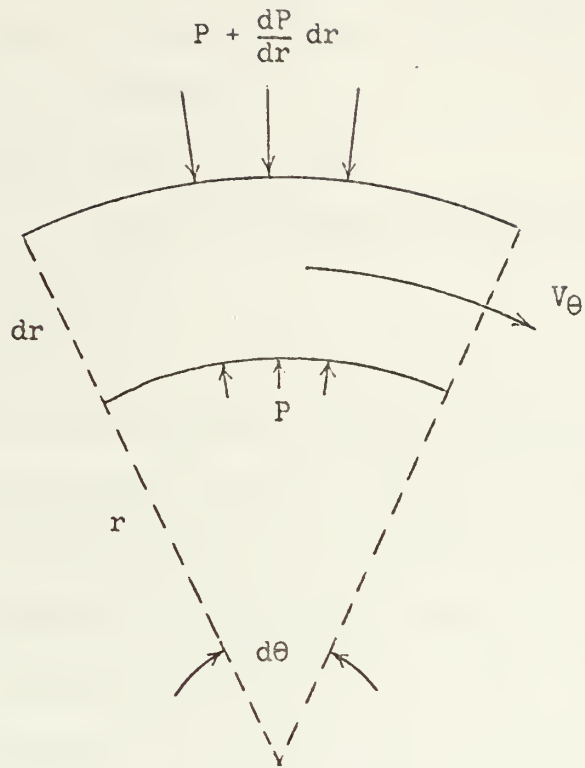
$$T \frac{\partial s}{\partial r} - \frac{\partial h_o}{\partial r} = V_x \frac{\partial V_r}{\partial x} - V_x \frac{\partial V_x}{\partial r} - V_\theta \frac{\partial V_\theta}{\partial r} - \frac{V_\theta^2}{r}. \quad (2.22)$$

At this point $\partial s/\partial r$ and $\partial h_o/\partial r$ are often assumed to be zero. According to Horlock⁶ these two assumptions, which prove to be nearly true in practice, hold for the flow between blade rows of a reversible turbine in which delivered work and total pressure drop across the blade are the same at all radii. The term, $V_x \cdot \partial V_r/\partial x$, is called the streamline curvature term and is the cause of the difficulty, mentioned in the introduction, in obtaining a solution to equation (2.22).¹ In addition to assuming $\partial s/\partial r$ and $\partial h_o/\partial r$ are equal to zero, if it is assumed that V_r equals zero at the leading and trailing edges of a blade row, the streamline curvature term drops out and the partial derivatives can be replaced by ordinary derivatives, giving

$$V_x \frac{dV_x}{dr} = - V_\theta \cdot \frac{dV_\theta}{dr} - \frac{V_\theta^2}{r}. \quad (2.23)$$

Equation (2.23) is called the simple radial equilibrium equation.

A more direct derivation of the simple radial equilibrium equation, which may be more intuitive, can be developed from consideration of an infinitesimal volume of fluid in equilibrium with the external forces acting on it.¹ The details are shown in Figure 2-1, on the next page. The substitution for the $g_o/\rho(dP/dr)$ term proceeds as above.



Sum of forces in the radial direction = 0

$$r \cdot d\theta \left(P + \frac{dP}{dr} dr \right) - P \cdot r \cdot d\theta - \frac{v_{\theta}^2}{r} (\rho r \cdot d\theta \cdot dr) = 0$$

$$\frac{dP}{dr} r \cdot d\theta \cdot dr = \rho \frac{v_{\theta}^2}{r} r \cdot d\theta \cdot dr$$

$$\frac{1}{\rho} \frac{dP}{dr} = \frac{v_{\theta}^2}{r}$$

Figure 2-1

In summary, the simple radial equilibrium equation is valid for the following conditions:

- (1) ideal, incompressible fluid flow
- (2) axial symmetry
- (3) perfect gas law holds
- (4) $V_r = 0$ before and after blade rows
- (5) $dh_o/dr = 0$
- (6) $ds/dr = 0$

2.4.3 Solutions to the Simple Radial Equilibrium Equation

From equation (2.9) it can be seen that the work performed by an axial turbine is related to the tangential velocities before and after the rotor, $V_{\theta 1}$ and $V_{\theta 2}$, respectively. A design problem for an axial turbine is to propose a reasonable tangential velocity distribution which will give the desired work, and then by means of the simple radial equilibrium equation find the axial velocity, V_x , so that the blade shapes can be determined. For simple functions of $V_\theta = V_\theta(r)$, equation (2.23) is easily integrated directly for $V_x = V_x(r)$.

It would appear that independent functions for $V_{\theta 1}$ and $V_{\theta 2}$ could be chosen and corresponding functions $V_{x1}(r)$ and $V_{x2}(r)$ calculated from the simple radial equilibrium equation. However, the V_θ 's are related by the work relation, equation (2.9), and by the assumption, used in deriving the simple radial equilibrium equation, that the stagnation enthalpy, h_o , after each blade row, does not vary with radius.

A familiar, useful set of tangential velocities given by Carmichael and Lewis, and described by Horlock⁶, are the following:

$$V_{\theta 1} = ar^n + \frac{b}{r} \quad (2.24)$$

$$V_{\theta 2} = ar^n - \frac{b}{r} \quad (2.25)$$

where a , n , and b ($b > 0$) may be chosen by the designers. Then, from equation (2.9)

$$\frac{\dot{W}}{\dot{m}} = \frac{u}{g_o J} (V_{\theta 1} - V_{\theta 2}) = \frac{2\pi r N}{60 g_o J} (V_{\theta 1} - V_{\theta 2}),$$

and using equations (2.24) and (2.25)

$$\frac{\dot{W}}{\dot{m}} = \frac{2\pi r N}{60 g_o J} \left(\frac{2b}{r}\right) = \frac{4\pi N b}{60 g_o J}. \quad (2.26)$$

Equation (2.26) shows the work done (hence h_o) is independent of radius and has the proper sign for a turbine.

A modification of the set of tangential velocities (2.24) and (2.25) is considered in this thesis. Suppose a set of tangential velocities of the following form is given:

$$V_{\theta 1} = a_2 r^2 + a_1 r + a_0 + \frac{b_1}{r}, \quad (2.27)$$

$$V_{\theta 2} = a_2 r^2 + a_1 r + a_0 + \frac{b_2}{r}. \quad (2.28)$$

Here also the work is independent of radius, for

$$\frac{\dot{W}}{\dot{m}} = \frac{2\pi N}{60 g_0 J} (b_1 - b_2). \quad (2.29)$$

Here b_1 must be greater than b_2 if work is to be done by the turbine. The constant b_1 is virtually always positive, and b_2 is usually negative or zero. The advantage of allowing b_1 and b_2 to be different is to be able to provide for special cases such as free vortex, axial outflow ($a_2, a_1, a_0, b_2 = 0; b_1 \neq 0$).

Substituting an expression of the form of (2.27) into the simple radial equilibrium equation and integrating from reference point $V_{xi} = V_x(r_i)$ to point $V_x = V_x(r)$, the following expression for axial velocity is obtained (the details are in Appendix D):

$$\begin{aligned} V_x^2 = V_{xi}^2 - \frac{3}{2} a_2^2 (r^4 - r_i^4) - \frac{10}{3} a_1 a_2 (r^3 - r_i^3) \\ - (4a_0 a_2 + 2a_1^2) (r^2 - r_i^2) - 6(a_0 a_1 + a_2 b_1) (r - r_i) \\ - (2a_0^2 + 4a_1 b_1) \ln\left(\frac{r}{r_i}\right) + 2a_0 b_1 \left(\frac{1}{r} - \frac{1}{r_i}\right). \end{aligned} \quad (2.30)$$

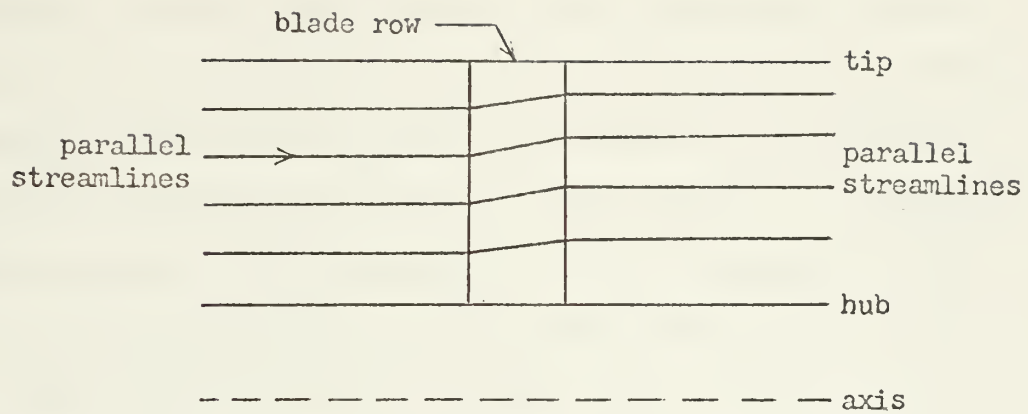
Equations (2.27) and (2.30) for tangential velocity and axial velocity form a set which satisfy the simple radial equilibrium equation (2.23). It is important to note that many factors and various criteria for good practice influence the detailed choice of the constants in the expressions for V_0 .

Two well known special cases of equations (2.27) and (2.28) are the constant reaction V_0 distribution and the exponential V_0 distribution. These tangential velocity distributions are presented in Appendix D together with the corresponding function for axial velocity.

2.5 Actuator Disk Theory

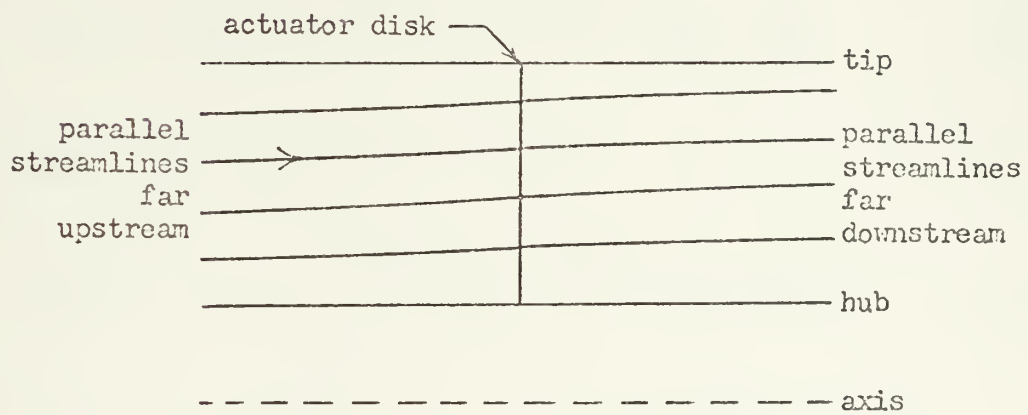
2.5.1 General

It is recalled that the basis for the simple radial equilibrium design method is that the radial component of the fluid velocity be zero at the leading and trailing edges of a blade row. This assumption results in streamlines of the form illustrated in Figure 2-2(a). A more general method of analysis, which takes some account of radial shifts in the streamlines between blades, is the actuator disk model. As described by Horlock⁶, a rotor or stator row is replaced, conceptually, at approximately midchord, by a thin disk across which the tangential velocity change takes place. Such a device allows the equations of motion, including radial velocity terms, to be solved analytically, although the formulation is still complex.



Simple Radial Equilibrium

(a)



Actuator Disk

(b)

Radial Flow Models

Figure 2-2

2.5.2 Approximate Solution

With some simplifications, an approximation to the complete actuator disk results can be obtained. Radial velocities are assumed to be zero at the walls and small elsewhere, and simple radial equilibrium is assumed to be valid a sufficient distance from the disk. According to this model, the streamlines will be similar to those shown in Figure 2-2(b). The approximate solutions for the axial velocity near a single disk, in terms of the axial velocity on the same streamline far up and downstream, are:

$$V_x(x) = (V_x)_{-\infty} + \frac{(V_x)_{+\infty} - (V_x)_{-\infty}}{2} \exp\left(\frac{\pi x}{h}\right), \quad (2.31)$$

upstream of the disk ($x < 0$), and

$$V_x(x) = (V_x)_{+\infty} - \frac{(V_x)_{+\infty} - (V_x)_{-\infty}}{2} \exp\left(-\frac{\pi x}{h}\right), \quad (2.32)$$

downstream of the disk ($x > 0$). The notation $(V_x)_{+\infty}$ and $(V_x)_{-\infty}$ refer to the axial velocities given by simple radial equilibrium a long way downstream and upstream, respectively; h is the height of the actuator disk.

This analysis, like the simple radial equilibrium analysis described in the previous section, treats ideal, incompressible flow in cylindrical annuli.

For real turbines, where many rows of blades (disks) may influence the axial velocity distribution, the effects of each disk may be considered separately, then superimposed to find the real axial velocity.¹ This procedure is used in Appendix E to find the axial velocity distribution at a point influenced by two nearest adjacent disks.

2.6 Flow in Flared Annuli

2.6.1 General

In addition to improving the methods for cylindrical flow, efforts to understand the fluid flow in ducts of changing annular cross-section have been made. Such sections are commonly used in practice.

Horlock, in reference 6, describes some theoretical models, proposed by various workers, for the determination of axial velocity. Analyses by Lewis and Horlock for incompressible flow in conical ducts, by Wu for compressible flow in flared annuli, and a simplification of Wu's analysis by Walker are discussed. The drawback of these analytical methods is their complexity.

Experimental work by Carmichael and Pai² has suggested a simple expression relating the axial velocity of flow in a flared duct to the angle the streamline makes with the axis. Their work, described below, forms the basis of the flare correction to axial velocity given in this thesis.

2.6.2 Experiments Representing Fluid Flow in Flared Turbines²

Experiments were conducted using a tilted-floor electrolytic tank to measure flows within a flared annulus. An electrolytic tank provides an analogue to ideal incompressible fluid flow. Electrical potential measured in the tank is analogous to fluid potential and the electrical potential gradient is analogous to the fluid velocity. A sector of an axisymmetric model can be represented by tilting the floor of the tank.

Although flow in a real turbine is compressible, the radial variation in density at any axial station is relatively small. Consequently, it can be assumed that in usual geometries the streamline positions for the real, compressible fluid are very nearly the same as for the ideal, incompressible case.

One aspect of the fluid flow measured was the general change in axial velocity distributions in the flared annulus. Three models were studied, with different distributions of flare between the hub and shroud walls; each model had a hub-tip ratio of 0.9. The distribution was expected to be a function of location within the annulus, described by an angle, ϕ , defined as shown in Figure 2-3. The flow conditions were measured at an axial position, free of discontinuities, such as section A-A' in Figure 2-4. The axial velocities were found to have the distribution shown in Figure 2-5,

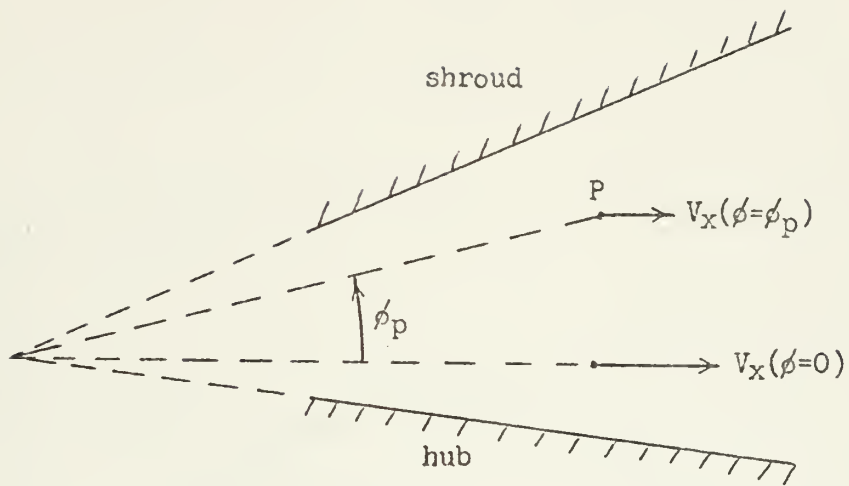


Figure 2-3

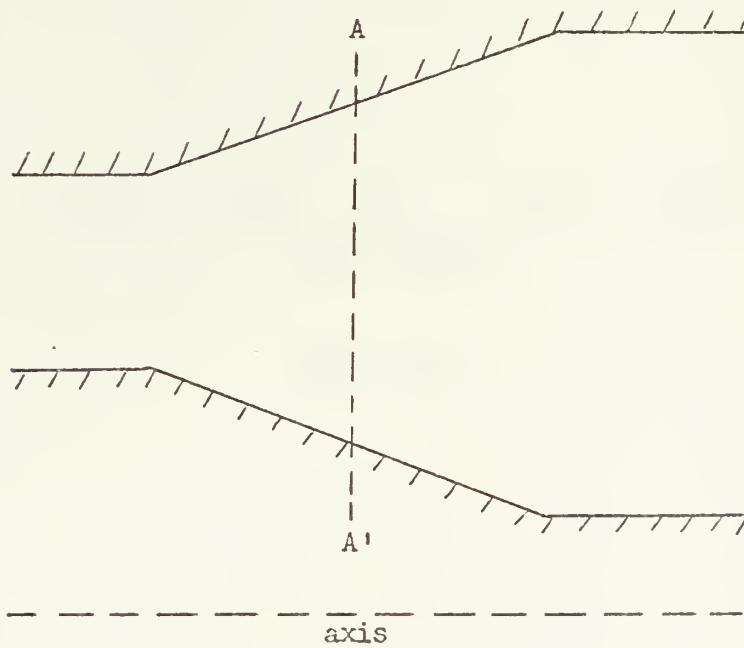


Figure 2-4

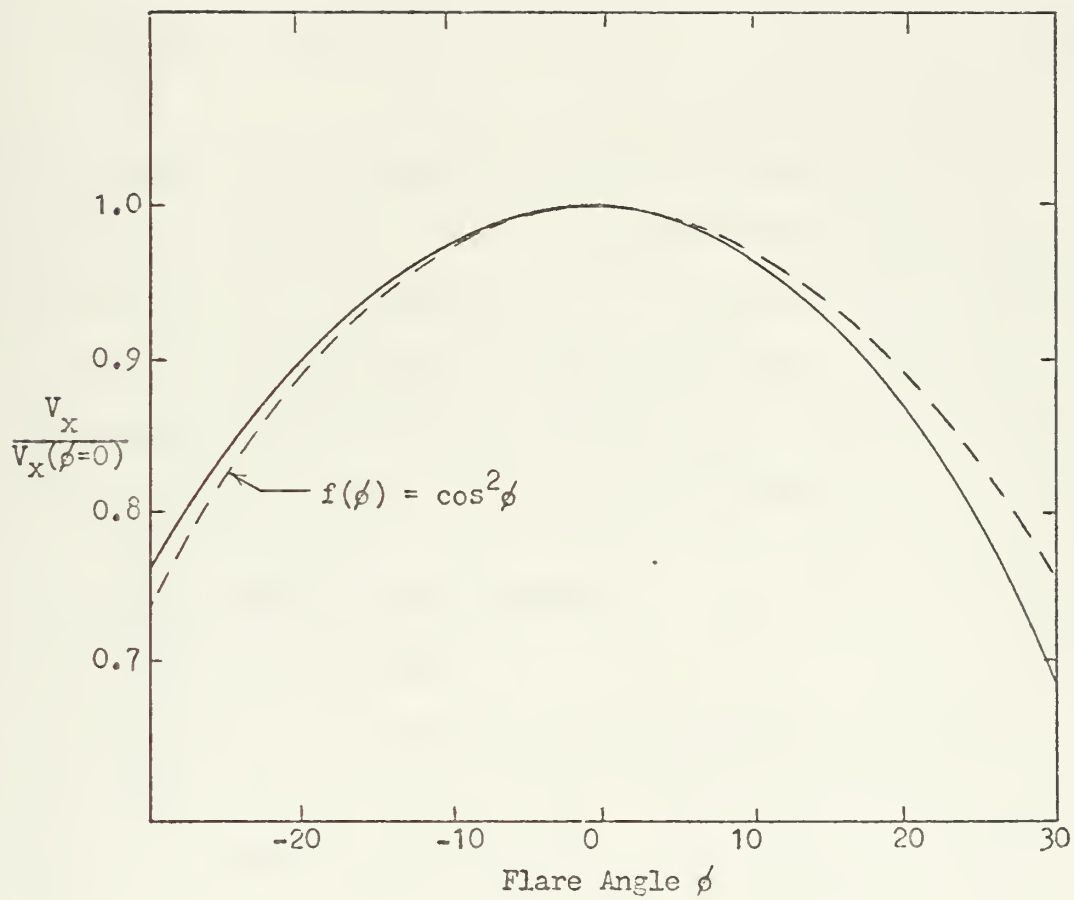


Figure 2-5

approaching the flow from a source. The equation, according to potential flow theory, for the axial velocity distribution for a two-dimensional source is

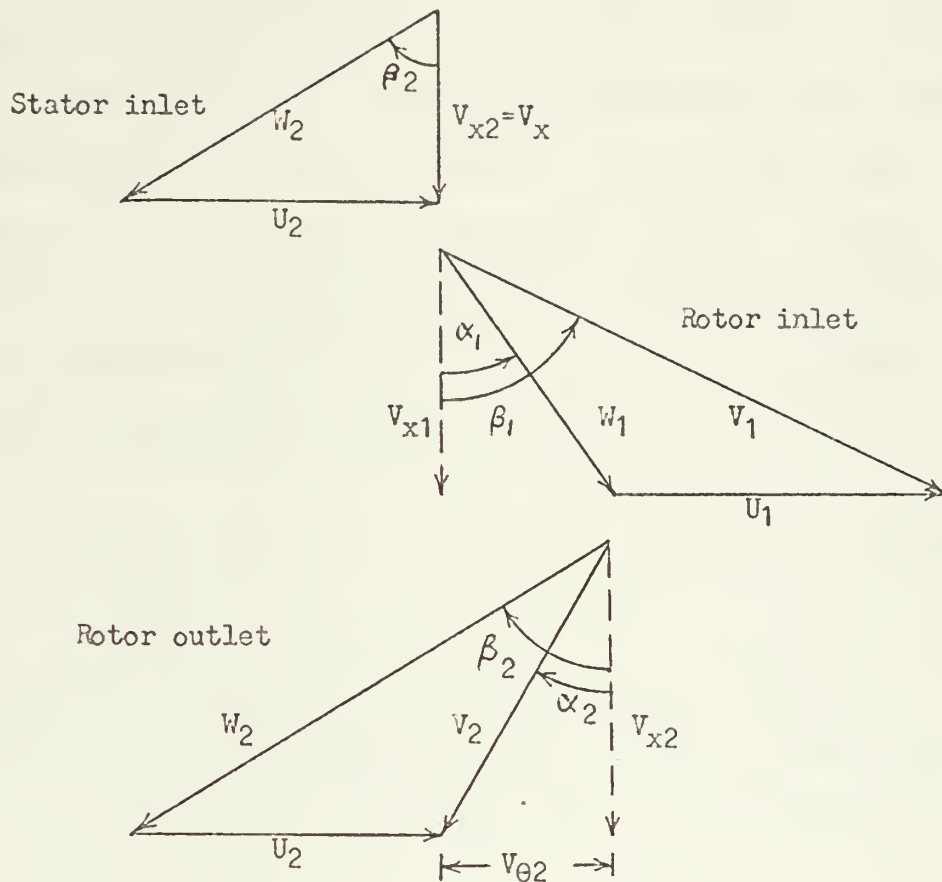
$$\frac{V_x}{V_x(\phi=0)} = \cos^2 \phi. \quad (2.33)$$

Pai suggests that comparison of this equation, also plotted in Figure 2-5, with the experimental results, indicates that for angles of $\phi < \pm 15^\circ$, equation (2.33) is a good representation of the axial flow. Even at larger angles, the agreement may be good enough to use equation (2.33) for some design applications.

2.7 Axial Turbine Flow Geometry

2.7.1 Velocity Triangles

It should be restated that the purpose of determining the details of the fluid flow is to be able to design the blades appropriately. The relevant fluid velocities and flow angles are conveniently displayed in the form of vector diagrams, often called velocity triangles. Velocity triangles for a single stage axial turbine with pure axial inflow are shown in Figure 2-6, where any radial velocity components have been neglected. The calculation of such velocity triangles for each leading and trailing edge and at several radii must be accomplished before the detailed design of the turbine blading can continue.



Remarks:

1. the signs of velocity components are positive in the direction of U or V_x
2. angles are positive in a counterclockwise direction from V_x
3. as drawn above--

$V_{\theta 1}, \alpha_1, \beta_1$ are positive
 $V_{\theta 2}, \alpha_2, \beta_2$ are negative

Figure 2-6

2.7.2 Annulus Area

Suppose a fluid is flowing uniformly through a small area at a given rate. If the area encompassing the flow is perpendicular to the streamlines, it is termed the flow area, A , and is given by equation (2.18). If the area is in a surface whose perpendicular makes an angle α to the streamlines, as in Figure 2-7, then the area required to encompass the same flow is

$$A_{\text{ann}} = A / \cos \alpha. \quad (2.34)$$

In the case of an axial flow turbine, A_{ann} represents the annulus flow area perpendicular to the machine axis, where α is the same α as in Figure 2-6. From Figure 2-7 it can be seen that

$$\cos \alpha = V_x / V;$$

whence equation (2.18) becomes

$$A_{\text{ann}} = \frac{\dot{m}}{\rho V_x}. \quad (2.35)$$

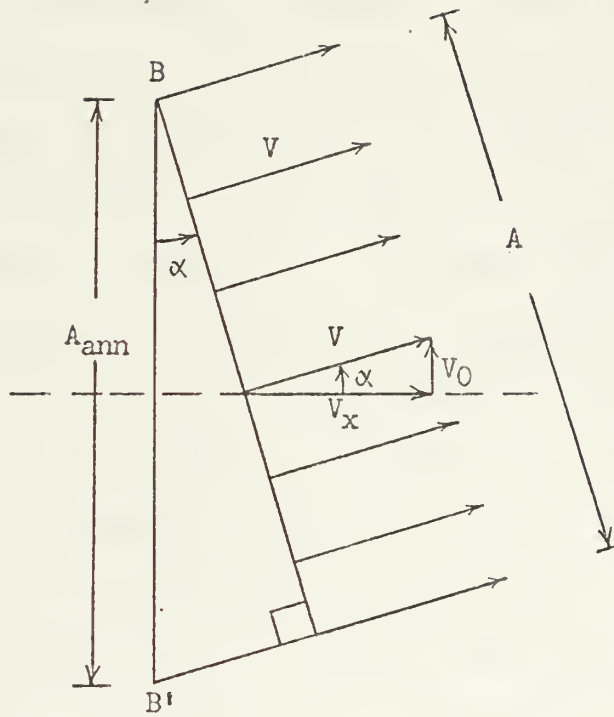


Figure 2-7

3. MODEL DESCRIPTION AND IMPLEMENTATION

3.1 General

In the introductory chapter the need for a simple methodology to generate a preliminary axial turbine design, taking account of turbine flare and radial streamline shifts, was discussed. The simple radial equilibrium design method was presented in Chapter Two, together with the results of actuator disk theory and axial flow distribution studies in flared annuli. In this thesis a procedure is proposed which accepts a simple radial equilibrium preliminary design as a basis, and then modifies the axial velocity distribution in accordance with the actuator disk and flare corrections mentioned above. These modifications to the simple radial equilibrium flow solution result in slightly different blade shapes, which should be more commensurate with the real flow.

This chapter will present the model for modifying a simple radial equilibrium preliminary design, and describe a computer program which implements the model.

3.2 Model Description

To begin, it is useful to consider a sketch of the geometry and then a bare outline of the problem.

Figure 3-1 represents a single stage axial flow turbine. The stator inlet, rotor inlet, and rotor outlet planes are labeled 1, 2, and 3 respectively. Other features will be discussed as they become important.

The following are steps in the procedure which may be identified in order to guide the discussion:

- (1) "input" a simple radial equilibrium preliminary design
- (2) at each of the three principal planes of the turbine stage, calculate a set of streamlines which is consistent with certain given conditions and the modified axial velocity
- (3) at every streamline in each principal plane, calculate velocity triangle data.

The rest of this section will discuss the above steps in general terms. The details of the procedure are best understood in the context of the computer program description, beginning in paragraph 3.3.

3.2.1 The Input Design

The purpose of the procedure discussed in this thesis is to make slight "corrections" in an existing simple radial equilibrium design in order to refine the detailed blade shapes. As a result of carrying out a preliminary design for a single stage, many parameters will have been established. The working fluid, total temperatures and pressures, hub and tip radii, machine rpm, mass flow, and blade widths are known; also, in the

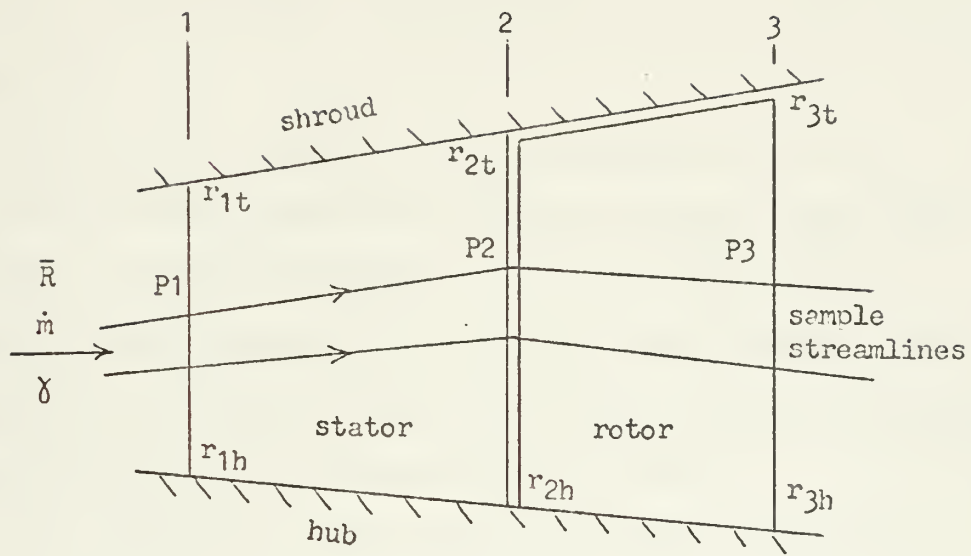


Figure 3-1

case of simple radial equilibrium, an appropriate pair of functions for axial and tangential velocity at each plane will have been picked. These quantities are indicated in Figure 3-1.

For present purposes, it is assumed that it is desired to retain the input annular geometry (hub and tip radii, and blade widths) in the modified case, although other choices are possible. For example, the average axial velocity could be fixed, and the tip radius allowed to change to accommodate the flow.

For simplicity, the input preliminary design is restricted to having hub and shroud surfaces of uniform slope over the whole stage, as in Figure 3-1. Also, the rotor tip clearance and stator-rotor gap are assumed to be zero. The model could be applied to more general cases with relatively minor modifications to the computer program. The turbine flare may be distributed between the hub surface and shroud surface in any proportion.

It should be noted that the procedure described here will, in no sense, improve a bad preliminary design.

3.2.2 Calculating the Streamlines

To fully determine the blade shape, fluid flow information, including axial velocity, must be known at several radii. If the design were merely simple radial equilibrium, the velocity triangles could be independently found at any convenient radius, since V_x and V_θ (and U) are known functions of r alone. However, in the present

case, the actuator disk correction to the axial velocity at a location on one plane is dependent upon the axial velocity along the same streamline at stations up and downstream. For this reason a set of streamlines passing all three principal planes must be calculated.

To find the final set of streamline positions, three different iterative loops are involved. They are:

- (1) at a given plane and streamline, iteration is required to obtain the next (radially outward) streamline position;

- (2) at a given plane, iteration is required to obtain an average axial velocity which will result in a match between the fixed mass flow rate and annulus area;

- (3) since a change in the axial velocity at a streamline in one plane affects the axial velocity in another plane, the streamlines are recalculated at each plane in succession until the changes from one iteration to the next become insignificant.

The modified axial velocity, used in the streamline calculations, is found utilizing the approximate actuator disk results described in paragraph 2.5 and Appendix E, and the flared annulus axial flow relation described in paragraph 2.6. The only changes to the simple radial equilibrium preliminary design are a result of these two "corrections" to the axial velocity, which impact on the velocity triangles. The changes represent a departure

from simple radial equilibrium. The justification for this procedure is that the adjustments are small and are improvements in the direction of the real solution.

3.2.3 Velocity Triangle Data

After the positions of streamlines have converged, all relevant parameters in the velocity triangles can be calculated from the primary variables U , corrected V_x , and V_θ , and input parameters. Other useful design data, for example, stator and rotor fluid turning angles and W_2/W_1 ratio, are easily derived from the basic velocity triangle data.

For purposes of comparison, sets of velocity triangles can be computed at the same streamline-plane locations, but using the unmodified simple radial equilibrium axial velocity.

3.3 Computer Implementation of the Model

3.3.1 General

The iterative nature of the detailed calculations virtually precludes hand calculations of the streamlines as a practical matter. A computer program to accomplish the calculations has been written in FORTRAN IV language making use of the model easy and inexpensive.

The goal of the work described in this thesis was to develop the model and to program it, so that it could be applied in future design studies. Since the model itself is experimental, the program is not merely

the mechanization of standard, accepted practice. For this reason, it was thought advisable to include here a sufficiently detailed description of the computer program so that the model used is clear and so that changes can be made easily in the future if desired. References 7 and 8 were useful as programming language guides.

The programming philosophy was to simplify the understanding and use of the program and to provide flexibility. The program was segmented into subprograms, each having a specific function. Identical variable labels have the same meaning in all segments of the program in order to simplify understanding it. The use of COMMON reduces the storage demands of the program. Extensive execution information, such as the number of loops performed and intermediate values can be printed out at the user's option. Diverging iterative loops are terminated by internal testing.

The following paragraph lists the significant steps in the execution of the program to modify a simple radial equilibrium design in accordance with the model. Subsequent paragraphs will discuss each step in detail.

3.3.2 Procedural Steps

The following list contains a list of all significant steps in the program. Some details, such as initialization of variables and testing for loop convergence, are omitted and are self-explanatory or can be conveniently discussed separately. Free use will be made of the

notation employed in the computer program itself. The list is intended to serve as a guide for the discussion; full appreciation of the interrelationships can be gained only by studying the program flow charts.

- (1) Read and process input data
- (2) At the first plane calculate a set of streamlines satisfying continuity using the simple radial equilibrium axial velocity corrected for flare
 - a) the first streamline follows the hub
 - b) guess at the location of the next streamline and iterate until continuity is satisfied between two streamlines
 - c) find locations of succeeding streamlines in turn until the last one has been calculated
 - d) compare the radial location of the last streamline to the desired tip diameter at the plane under consideration
 - e) if a discrepancy exists, modify the "average" axial velocity at that plane and repeat from a) above
- (3) Repeat (2) for planes 2 and 3
- (4) After a set of streamlines is calculated for all three planes, recalculate them all as before but using the actuator disk correction on the axial velocity as well

- (5) Test to see if the streamline positions for plane three have changed much; if they have, go back to step (4) and recalculate the streamline positions for all three planes
- (6) Calculate and print velocity triangle data for each streamline position at each plane, using the modified axial velocity
- (7) Repeat (6), but using the simple radial equilibrium axial velocity.

3.3.3 Overall Program

The overall program is represented by the flow chart in Figure 3-2, on the next page. The circled numbers provide points of reference for more specific flow charts in later figures. The initialization, incrementing, and printing of L1, L2, and L3 are included in the flow charts so that the user can readily interpret certain diagnostic output to be described later.

3.3.4 Reading and Processing Input Data

The first step in the program is to read a set of input data and perform some preliminary calculations. This is accomplished by the main program, MAIN.

The following is a list of the input, determined from a simple radial equilibrium design, which must be submitted:

- (1) working fluid, specific gas constant, and specific heat ratio

MAIN: Overall

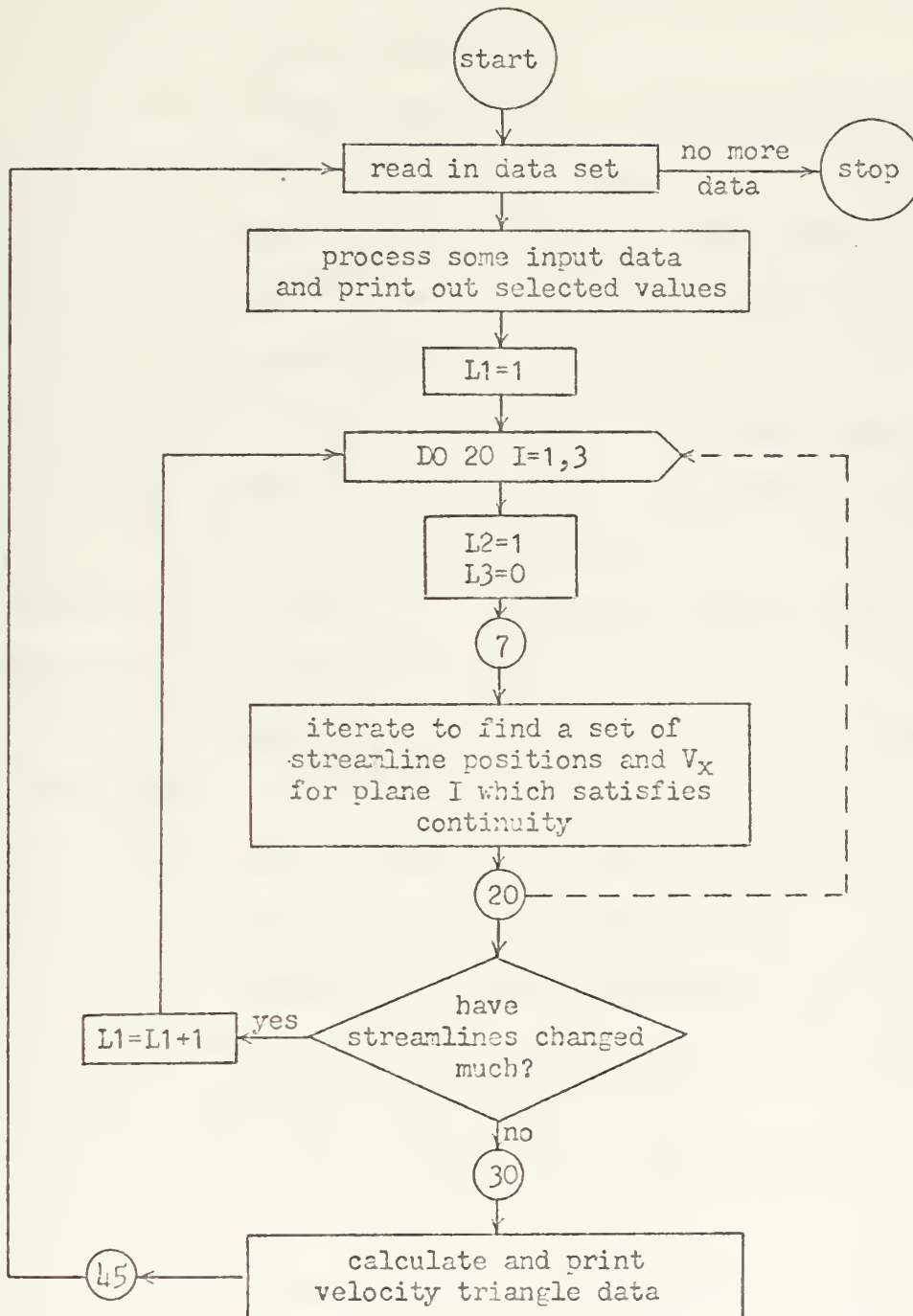


Figure 3-2

- (2) turbine mass flow rate and rpm
 - (3) total temperatures and pressures at all three planes
 - (4) hub and tip radii at planes one and three
 - (5) stator and rotor widths
 - (6) coefficients of terms in the simple radial equilibrium relation for tangential velocity at each plane
- and
- (7) a reference velocity and radius used to find the simple radial equilibrium axial velocity at each plane.

In addition, the number of streamlines desired and certain test values are read in.

The following calculations of a preliminary nature are performed:

- (1) test to ensure the overall flare is not zero and calculate flare angles
- (2) calculate the basic parameters used to apply the flare correction to the axial velocity (paragraph 3.3.9)
- (3) calculate dimensional test values from input (paragraph 3.3.13)
- (4) calculate blade heights
- (5) calculate certain other often used combinations of input which remain constant for the data set under consideration

Selected parameters are printed out prior to further execution of the program.

3.3.5 Calculating a Streamline Location

The heart of the whole program is the calculation of streamlines; the most basic step in the streamline generation is the calculation of the "next" streamline location, RNEXT, from the position of an adjacent streamline, R(I,J), and values VXZ and VTZ, representing average values of the axial and tangential velocities in the channel between RNEXT and R(I,J). This calculation is performed by subprogram RNEXT(I), whose flow chart appears in Figure 3-3.

The total velocity, V, is determined from the axial and tangential components, and with equation (2.13) determines the static to total temperature ratio. The temperature ratio and the equation of state for a perfect gas, equation (2.10), are used in another compressible flow relation, equation (2.17), to find a density RHO. Then the continuity equation (2.35) can be used to find a flow area, AREA. From

$$RNEXT = \sqrt{\frac{AREA}{\pi} + R(I,J)^2} \quad (3.1)$$

the location of the next radially outward streamline can be found.

Subprogram RNEXT

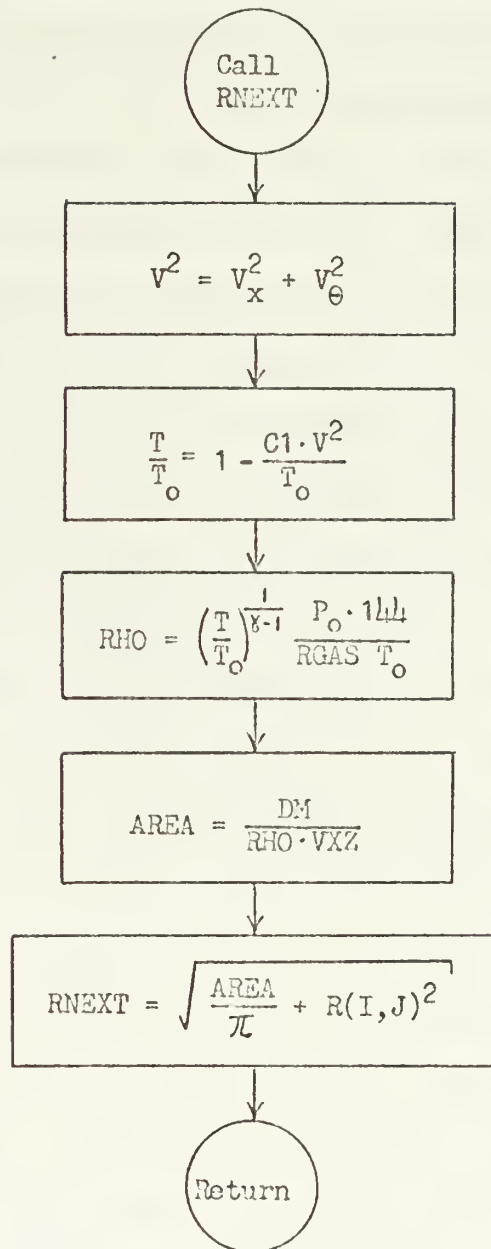


Figure 3-3

Since RNEXT depends upon average values of axial and tangential velocities, which are in turn functions of radius, iteration is required. This iteration is accomplished by the subroutine STREAM shown in Figure 3-4.

STREAM utilizes RNEXT as a guess for the next streamline and then calculates the average velocity values. The average values VXZ and VTZ are then used to calculate a new RNEXT and so on. When finally the difference between any RNEXT and the previous RNEXT is small, STREAM returns the values $R(I,J+1) = RNEXT$, $VX(I,J+1)$, and $VT(I,J+1)$ to the main program. The index L3 counts the number of times RNEXT is calculated during the calculation of a set of JJ streamlines at any plane.

In addition to finding an $R(I,J+1)$, STREAM also applies the flare and actuator disk corrections to the unmodified (simple radial equilibrium) axial velocity. The corrections are accomplished by multiplying the unmodified axial velocity, calculated in subprogram FVX(I) (paragraph 3.3.6), by the corrections for flare and actuator disk effects which are calculated by subprograms FLARE(I) and DISK(I), respectively. (See paragraphs 3.3.9 and 3.3.10) Since the very first time a set of streamlines is calculated at a plane, DISK is undefined, only the flare correction can be utilized in the first (L1=1) loop.

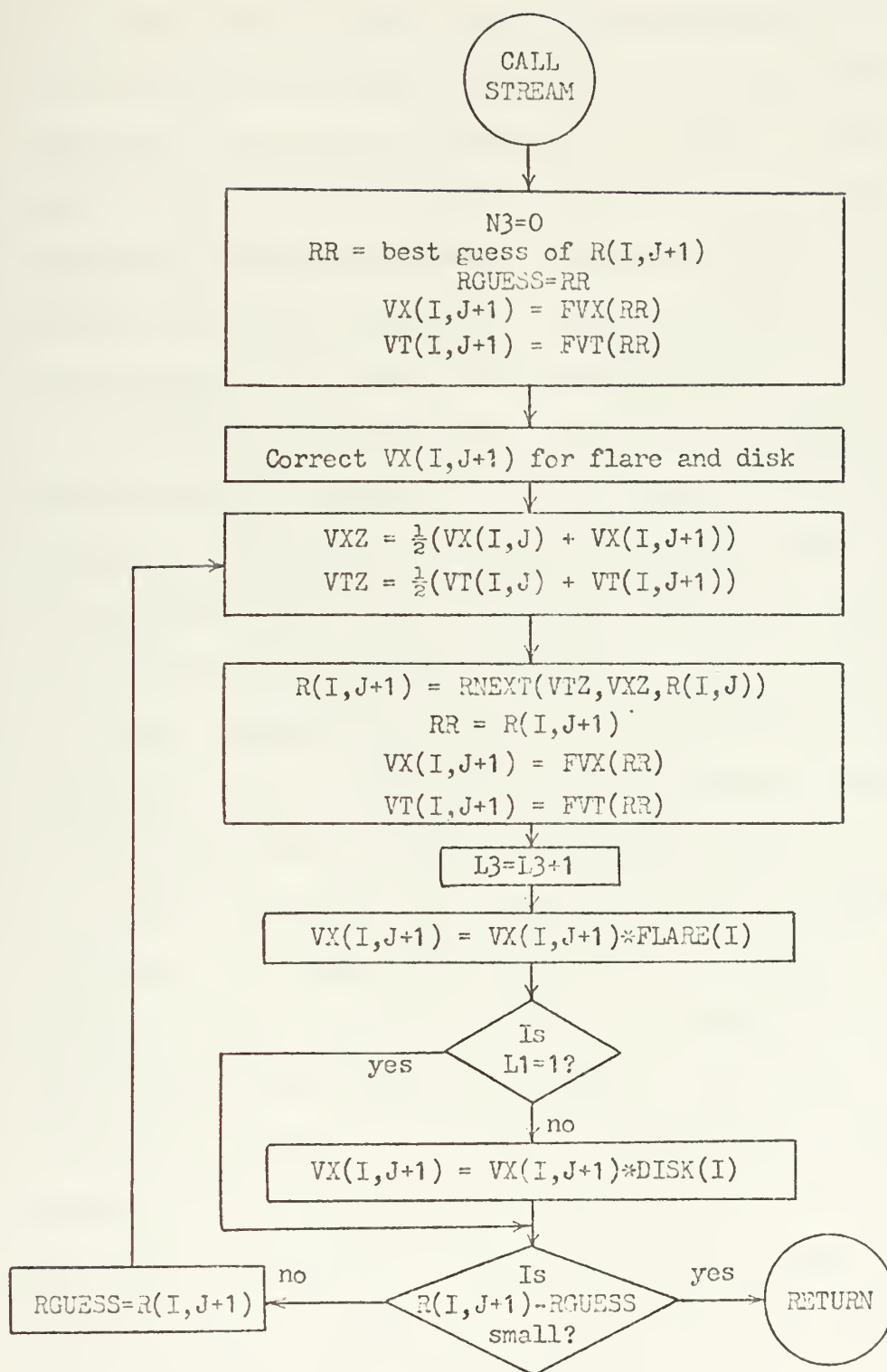


Figure 3-4

3.3.6 Calculating V_x and V_θ (Simple Radial Equilibrium)

In a simple radial equilibrium preliminary design, it is standard procedure to pick a functional form for the radial variation of tangential velocity. Then, the radial variation of the axial velocity is determined by the simple radial equilibrium equation (2.23). In the present case, the tangential velocity can have the form of equation (2.27) where the coefficients a_2 , a_1 , a_0 , and b are chosen by the designer. The simple radial equilibrium equation has been integrated for this form in Appendix D, resulting in equation (2.30). The function subprograms FVX(I) and FVT(I) calculate the simple radial equilibrium values of axial velocity and tangential velocity, respectively, given an argument RR and input parameters A2(I), A1(I), A0(I), B(I), VX0(I), and R0(I).

3.3.7 Generating a Feasible Streamline Set at a Plane

The main program calculates a set of streamline locations at a plane starting with the hub and using STREAM to step outward to the tip. Because the axial velocity has been modified, however, the average axial velocity is different from the simple radial equilibrium design value, and the last streamline does not fall on the fixed tip radius. To correct this, a reference axial velocity, VXR(I), used by FVX(I), is adjusted and the streamline set is recalculated.

The iteration is continued until the last streamline location is close enough to the desired tip radius. A flow chart of the section of MAIN that generates a set of streamlines that fit the geometry is shown in Figure 3-5. The variables S and S1 do not play a direct role in the streamline generation and will be explained in paragraph (3.3.11). The adjustment of the reference axial velocity is explained in the next paragraph. The index L2 counts the number of iterations made at a plane to converge to the proper R(I,JJ). At the users option (by specifying KK=1 in the input data) L2 and other parameters may be printed out after each trial set of streamlines.

3.3.8 Adjusting VXR(I)

Initially, VXR(I) is set to VXØ(I), the value determined from the simple radial equilibrium design. Whenever the location of the last streamline, R(I,JJ), misses the tip radius, RT(I), VXR(I) is adjusted to increase or decrease the average axial velocity before recalculating a new set of streamline locations, in order to make R(I,JJ) converge to RT(I).

To find an expression for a correction to the reference axial velocity in terms of the error, $DR = R(I,JJ) - RT(I)$, an expression for the flow

$$\frac{\dot{m}}{\rho} = V_x \cdot A \quad (3.2)$$

MAIN: Iteration for Streamlines at a Plane I

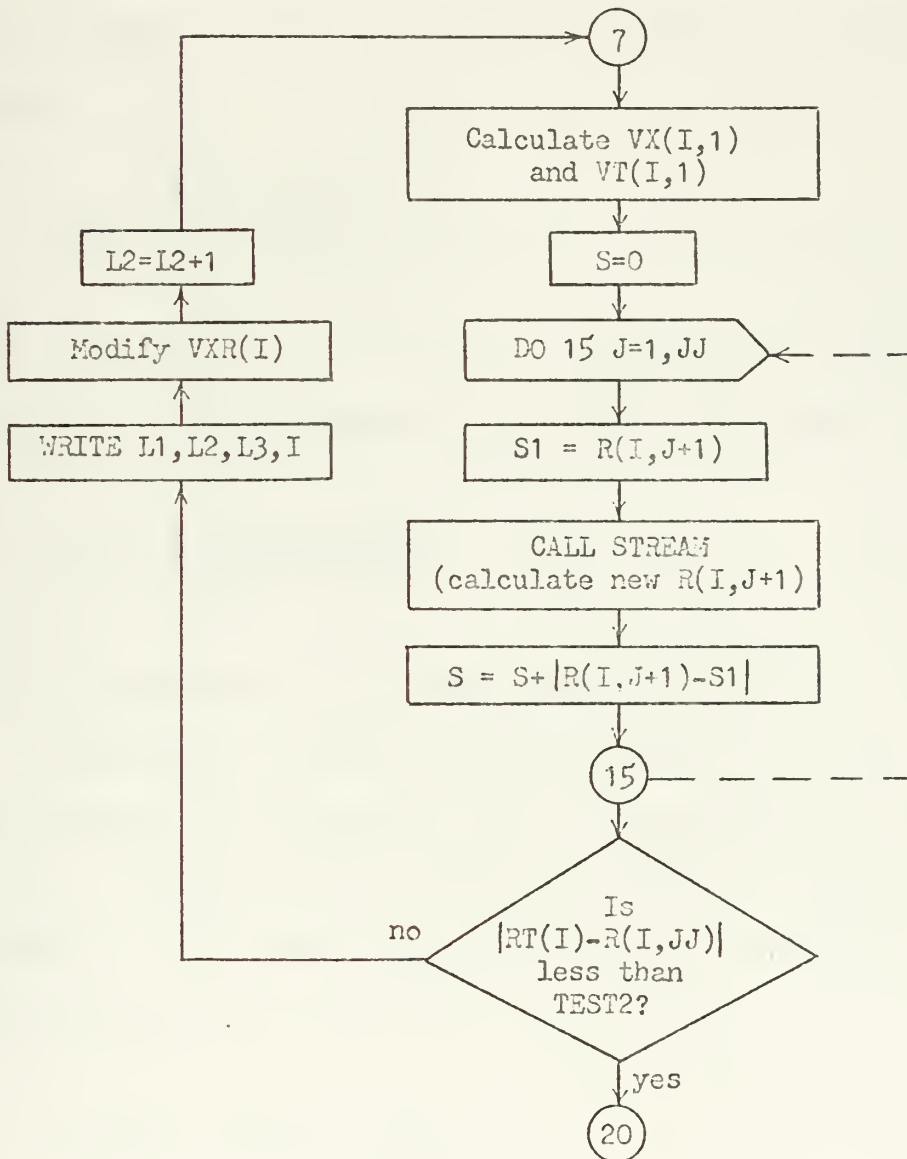


Figure 3-5

can be differentiated, giving ..

$$d\left(\frac{\dot{m}}{\rho}\right) = A dV_x + V_x dA. \quad (3.3)$$

But we desire $d(\dot{m}/\rho) = 0$ and $A = \pi(RT(I)^2 - R(I,l)^2)$
whence

$$dV_x = \frac{2V_x RT(I) \cdot DR}{RT(I)^2 - R(I,l)^2}. \quad (3.4)$$

From experience, to make the convergence more rapid, the following term was added to the VXR(I) by MAIN:

$$dV_x = \frac{2 V_x(I,JJ) DR}{RT(I) - R(I,l)} \quad (3.5)$$

3.3.9 Correcting Axial Velocity for Flare

The simple radial equilibrium axial velocity calculated by subprogram FVX(I) is corrected by multiplying it by a non-dimensional factor computed by subprogram FLARE(I). The basic relation involved is equation (2.33), rewritten as

$$FLARE = \cos^2 \phi = \frac{1}{\tan^2 \phi + 1}, \quad (3.6)$$

where

$$\tan \phi = \frac{RR - REF}{D}. \quad (3.7)$$

RR is the radial location of the point of interest, D is a parameter depending upon the plane under consideration, and REF is a geometric parameter. For additional details see Appendix F. FLARE is always positive and less than or equal to one.

3.3.10 Correcting Axial Velocity for Actuator Disk Effects

The actuator disk correction is applied after the flare correction and is also a multiplicative non-dimensional factor, calculated by subprogram DISK(I). The relations used in DISK(I) are forms of equations (E.1), (E.5), and (E.2) for planes one, two, and three, respectively. DISK is always positive and may be greater than one.

3.3.11 Testing for Overall Streamline Convergence

The corrected axial velocity at a streamline depends upon its location and the value of axial velocity on the same streamline at planes up and downstream. Therefore, in general it is necessary to recalculate the streamlines at each plane several times, the streamlines moving less with each iteration. The streamline positions are calculated in order at planes one, two, and three at least twice. Each time the streamlines for plane three are recalculated, the following sum is accumulated:

$$S = \sum_{J=1}^{JJ} |R(3,J)_{\text{this iteration}} - R(3,J)_{\text{last iteration}}|$$

(3.8)

Refer to Figures 3-2 and 3-5. If S is small enough, the streamline positions have not changed much from the previous iteration. This means that the set of corrected axial velocities, $VX(I,J)$, and streamline positions, $R(I,J)$, have converged to mutually consistent values, and iteration can be terminated.

3.3.12 Velocity Triangle Calculations

Once the streamlines have been located at each principal plane, a velocity triangle can be constructed at each point. P1, P2, and P3 in Figure 3-1 are the three points for one particular streamline. JJ triangles are constructed at each plane.

The fundamental input variables to the velocity triangle calculations are the streamline location $R(I,J)$, $VT(I,J)$, and $VX(I,J)$, which were calculated concurrently in the iteration process. The following derived quantities were calculated by MAIN at each plane:

$$U = 2\pi \cdot \text{RPM} \cdot R(I,J)/60 \quad (3.9)$$

$$V = \sqrt{VT(I,J)^2 + VX(I,J)^2} \quad (3.10)$$

$$W = \sqrt{VX(I,J)^2 + [U - VT(I,J)]^2} \quad (3.11)$$

$$\alpha = \arctan\left(\frac{VT(I,J)}{VX(I,J)}\right) \quad (3.12)$$

$$\beta = \arctan\left(\frac{VT(I,J) - U}{VX(I,J)}\right) \quad (3.13)$$

M = from equation (2.16)

$$M_{rel} = M \cdot \frac{W}{V} \quad (3.14)$$

In addition, the following quantities were calculated for each streamline:

$$\frac{V1}{V2} = \frac{V(\text{plane } 2)}{V(\text{plane } 1)} \quad (3.15)$$

$$\frac{W2}{W1} = \frac{W(\text{plane } 3)}{W(\text{plane } 2)} \quad (3.16)$$

$$\text{stator turning angle} = \alpha(\text{plane } 2) - \alpha(\text{plane } 1) \quad (3.17)$$

$$\text{rotor turning angle} = \beta(\text{plane } 3) - \beta(\text{plane } 2) \quad (3.18)$$

To compare the above results to those attainable by simple radial equilibrium, all of the above velocity triangle calculations are repeated at the same locations, but with the unmodified simple radial equilibrium axial velocity.

Figure 3-6 is a flow chart describing the calculation and printing of the above results.

3.3.13 Iteration Test Values

For flexibility, the user supplies the test values used to terminate the three iteration loops. The three loops are (1) overall streamline convergence,

MAIN: Calculate and Print Velocity Triangles

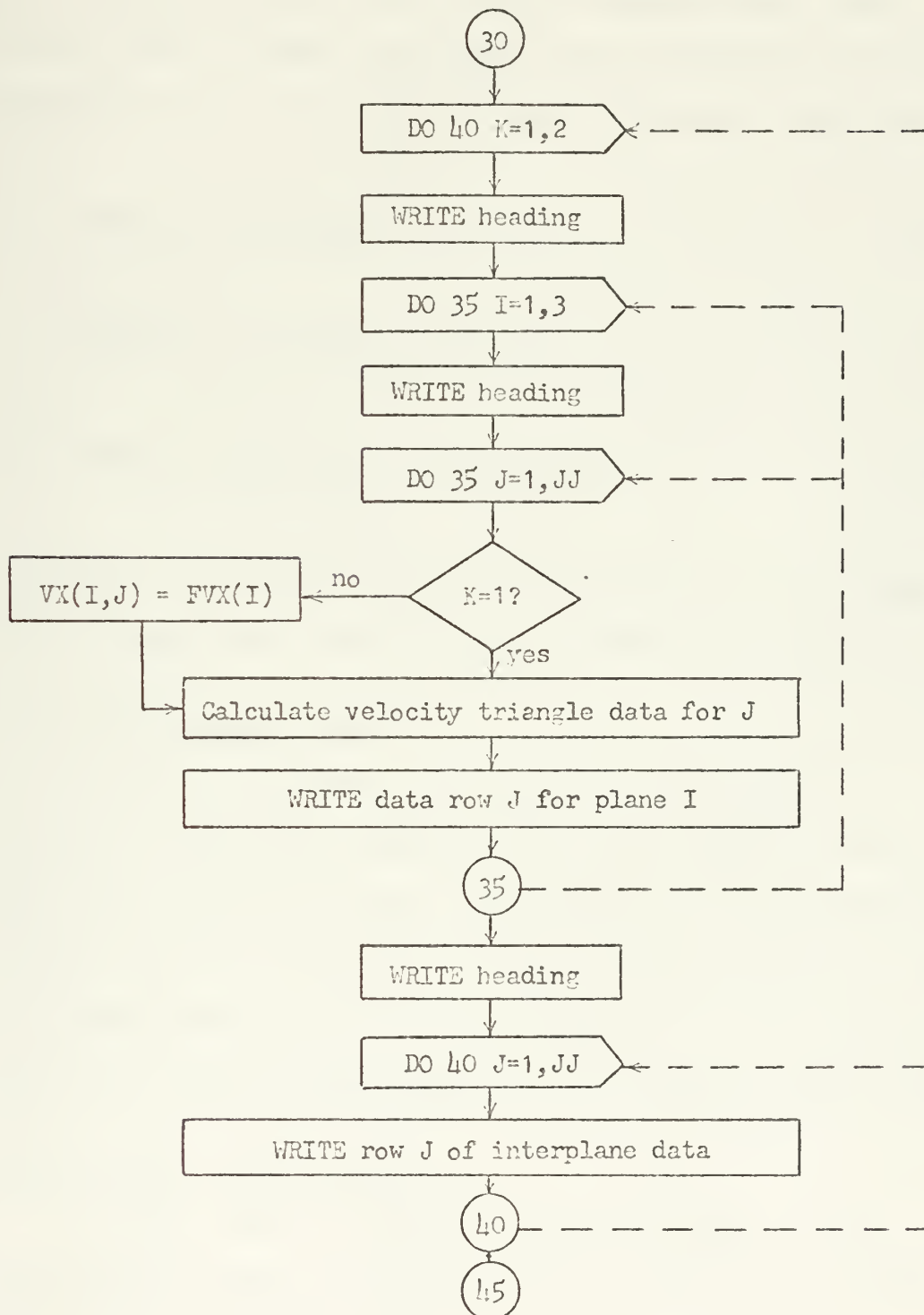


Figure 3-6

(2) convergence of the JJ'th streamline at a plane to RT(I), and (3) the location of the next streamline R(I,J + 1). These three loops are counted and labeled by the variables L1, L2, and L3, respectively. Test values TEST1, TEST2, and TEST3 are calculated from input parameters T1, T2, and T3 and the following relations:

$$\text{TEST1} = \text{T1} (\text{RT}(2) - \text{R}(2,1)) \quad (3.19)$$

$$\text{TEST2} = \text{T2} (\text{RT}(2) - \text{R}(2,1)) \quad (3.20)$$

$$\text{TEST3} = \text{T3} (\text{RT}(2) - \text{R}(2,1))/\text{JM1} \quad (3.21)$$

An iteration loop is terminated normally when the error term becomes less than the appropriate test value.

3.4 Convergence Checks

If for some reason the program ever begins to calculate diverging values of the error term in any of the three iteration loops, the program will automatically terminate the calculations on the current data set. This is accomplished, as depicted in Figure 3-7, by exiting if the error term has increased at least twice in that loop.

3.5 Program Verification

In this thesis a model to improve simple radial equilibrium design by applying flare and actuator disk corrections to axial velocity is described and a

Test for Loop Divergence

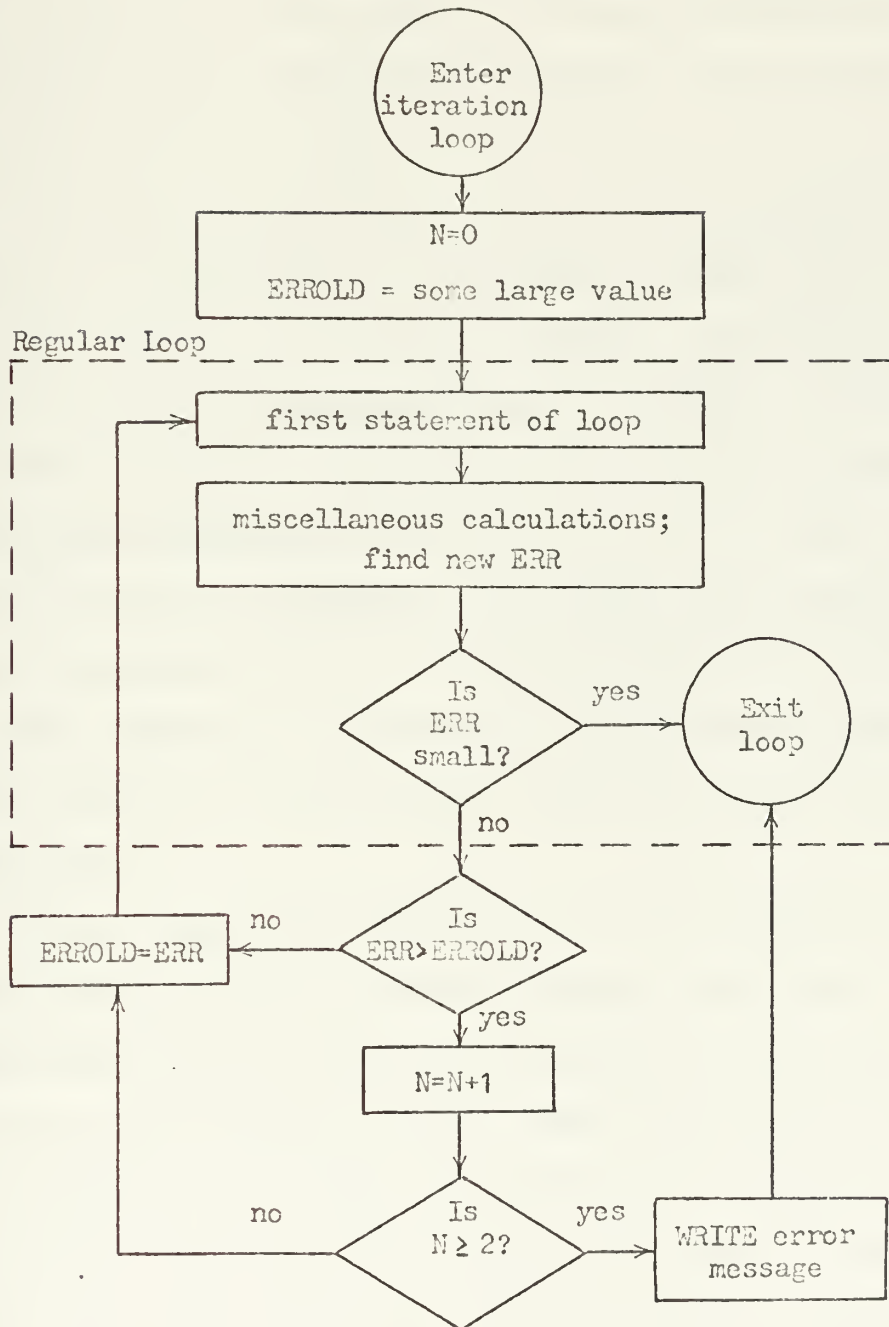


Figure 3-7

computer program to implement the model is presented. The computer program has been verified to the extent that there is confidence that it accurately reflects the model. Full evaluation of the model, including comparison to more complicated, exact design methods, must be left for future efforts.

Although the iterative nature of the streamline calculations makes hand calculation of the whole procedure very burdensome, it is easy to verify a solution by hand. The outputs of subprograms FLARE(I), DISK(I), FVX(I), and FVT(I) were all verified by hand, given a computer calculated streamline position $R(I, J + 1)$. With these values and $R(I, J)$, RNEXT(I) and STREAM were verified by hand calculating $R(I, J + 1)$. The computer calculations of flare geometry, velocity triangle related output, and other algebraic relationships, all agreed with hand calculation.

Since each input data set must be a complete simple radial equilibrium preliminary design, the number of independent geometries, working fluids, tangential velocity distributions, etc., tested was not very large. Nevertheless, it is felt the verification of the program was sufficient to ensure accuracy for feasible designs. Results are shown for three sample cases in Chapter 4.

4. RESULTS

4.1 General

This chapter presents the results of applying the computer program to three sample simple radial equilibrium designs. The computer output listing is included and plots of representative variables are provided for easy comparison between the simple radial equilibrium input design and the modified design.

4.2 Free Vortex Design

Table 4-1 shows the characteristics of an axial inflow and outflow free vortex stage designed as the last stage of a double flow turbine in a geothermal power application.⁹ A sketch of the geometry appears in Figure 4-2. Notice the design has a constant hub radius, but has large flare in the shroud. The working fluid is Freon 21. Eleven streamlines are called for.

The computer printed results are listed in Tables 4-3, 4-4, and 4-5. It is seen that the large changes in axial velocity (about 25% at the hub) can result in a six degree change in the relative inflow angle to the rotor. Less pronounced, but readily noticed changes are shown in other flow angles, velocity ratios, and Mach numbers.

In Figure 4-6, the axial velocity, stator outlet angle, rotor fluid turning angle, and relative velocity ratio are plotted for both modified and original simple radial equilibrium designs. It may be significant to note that the changes at the hub (where $\phi = 0^\circ$) may be considered to be "indirect" in that they result from the increased average axial velocity required to obtain the same mass flow.

4.3 Constant Reaction Design

The input parameters for another example having the same annular geometry as above but with a different assumed tangential velocity distribution are shown in Table 4-7. Axial inflow to the stage is maintained, but the constant reaction type simple equilibrium relations (see Appendix D) are used at the rotor leading and trailing edges.

The computer printed results are shown in Tables 4-8, 4-9, and 4-10, and plots of axial velocity and rotor relative flow angles appear in Figure 4-11. From Figure 4-11, the modification to axial velocity doesn't seem as significant as in the first example; the influence on the rotor flow angles is still significant, however ($\Delta\beta = 6^\circ$ at the hub).

4.4 Free Vortex, High Mach Number Design

To demonstrate the adequacy of the computer program to calculate in regimes where $M \geq 1.0$, the preliminary design summarized by Table 4-12 was run. In this case, the flare is symmetrically distributed between hub and shroud, as is shown in Figure 4-13.

The detailed results are listed in Tables 4-14, 4-15, and 4-16. The axial velocity and Mach number at the rotor inlet (plane 2) are plotted in Figure 4-17 for comparison with the simple radial equilibrium values.

SIMPLE RADIAL EQUILIBRIUM PRELIM TURBINE DESIGN
WITH FLARE AND ACTUATOR DISK CORRECTIONS

INPUTS

GAMMA=	1.1300	HS=	0.245000
RGAS=	10.9000	HR=	0.307000
RPM=	3000.000	TEST1=	0.002760
FLOW=	284.5000	TEST2=	0.001380
REF=	0.907000	TEST3=	0.000138
WF=	0.286482	TEST4=	0.000140
WS=	0.083000	WR=	0.083000
PHITIP=	36.7594	PHIHUB=	0.0000
JJ=	11		

PLANE	1	2	3
TA(I)	588.0000	588.0000	550.0000
PA(I)	60.0000	60.0000	33.6000
RT(I)	1.120999	1.183000	1.245000
R(I,1)	0.907000	0.907000	0.907000
RA(I)	0.907000	0.907000	0.907000
VX0(I)	164.0000	158.0000	164.0000
B(I)	0.00000	327.69995	0.00000
A0(I)	0.00000	0.00000	0.00000
A1(I)	0.00000	0.00000	0.00000
A2(I)	0.00000	0.00000	0.00000

Table 4-1

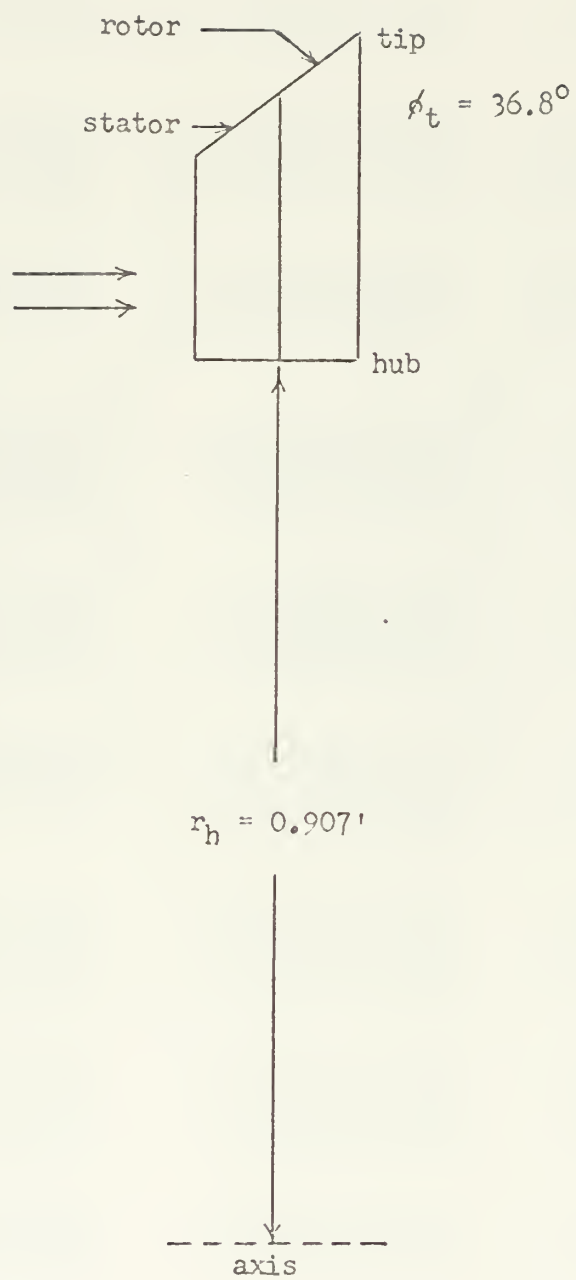


Figure 4-2

RESULTS FOR SRE MODIFIED HY FLARE, DISK

PLANE NO. 1 VXR(1)= 101.8114

J	R	U	VX 2	VT 2	V 2	W 2	ALPHA 2	BETA 2	MV 2	TH 2
1	0.90700	284.942	193.53328	0.00000	193.53320	344.45215	0.0000	-55.8154	0.40303	0.71732
2	0.92754	291.401	192.49466	0.00000	192.49487	349.23090	0.0000	-56.5510	0.40085	0.72725
3	0.94785	297.775	189.52557	0.00000	189.52551	352.02200	0.0000	-57.0243	0.39460	0.73491
4	0.96805	304.121	184.85400	0.00000	184.85486	355.89380	0.0000	-58.7074	0.38474	0.74081
5	0.98833	310.493	178.72384	0.00000	178.72302	358.25732	0.0000	-60.0742	0.37190	0.74549
6	1.00886	316.942	171.37186	0.00000	171.37183	360.30640	0.0000	-61.4597	0.35648	0.74949
7	1.02979	323.916	163.03934	0.00000	163.03931	362.27661	0.0000	-63.2537	0.33951	0.75325
8	1.05120	330.270	153.95180	0.00000	153.95178	364.38867	0.0000	-65.0079	0.32103	0.75734
9	1.07352	337.256	144.32114	0.00000	144.32104	366.83765	0.0000	-66.83326	0.30085	0.76216
10	1.09668	344.533	134.34303	0.00000	134.34375	369.79883	0.0000	-68.64977	0.27901	0.76801
11	1.12097	352.164	124.19713	0.00000	124.19713	373.42310	0.0000	-70.55739	0.25578	0.77525

PLANE NO. 2 VXR(2)= 203.4130

J	R	U	VX 1	VT 1	V 1	W 1	ALPHA 1	BETA 1	MV 1	TH 1
1	0.90700	284.942	197.60544	427.45288	470.91821	243.63342	65.1896	35.7087	1.0721	0.52105
2	0.92681	294.308	196.43573	413.85083	458.10425	229.95117	64.6045	31.3231	0.87807	0.46095
3	0.94528	303.251	193.15715	401.64575	445.57847	216.77490	64.3164	26.9944	0.73054	0.44205
4	0.96281	311.909	188.10605	390.49609	433.44141	203.86279	64.2793	22.6740	0.62741	0.43384
5	1.01484	320.391	181.60255	380.15894	421.30786	191.18506	64.4661	18.2172	0.49422	0.42624
6	1.04556	328.785	173.93935	370.45264	409.25537	178.86047	64.8464	13.4714	0.4134	0.37951
7	1.07325	337.172	165.78633	361.23828	397.29810	167.12817	65.4002	8.2794	0.34179	0.35411
8	1.10015	345.622	156.18405	352.40649	385.46606	156.33215	66.0973	2.4874	0.28161	0.33079
9	1.12747	354.204	146.54770	343.86841	373.79370	146.91162	66.9176	-4.00341	0.23003	0.31045
10	1.15541	362.983	136.66170	335.55103	362.31323	139.38733	67.8402	-11.3502	0.17647	0.29419
11	1.18420	372.028	126.68663	327.33282	351.04032	134.31982	68.8458	-19.44080	0.14077	0.28317

PLANE NO. 3 VXR(3)= 192.9946

J	R	U	VX 2	VT 2	V 2	W 2	ALPHA 2	BETA 2	MV 2	TH 2
1	0.90700	284.942	194.50221	0.00000	194.50220	344.99756	0.0000	-55.6824	0.41093	0.74314
2	0.94114	295.668	193.38445	0.00000	193.38440	353.29419	0.0000	-56.8113	0.41055	0.74100
3	0.97439	306.113	190.22943	0.00000	190.22937	360.40576	0.0000	-58.1417	0.40068	0.77618
4	1.00710	316.389	185.33630	0.00000	185.33630	366.67554	0.0000	-59.6384	0.39083	0.78046
5	1.03950	326.595	178.99913	0.00000	178.99902	372.43066	0.0000	-61.2739	0.38026	0.80157
6	1.07213	336.819	171.49805	0.00000	171.49805	377.96606	0.0000	-63.0162	0.36907	0.81317
7	1.10490	347.142	163.09507	0.00000	163.09497	383.54492	0.0000	-64.83348	0.35774	0.82482
8	1.13841	357.642	154.02823	0.00000	154.02856	389.39341	0.0000	-66.64995	0.34110	0.83705
9	1.17265	368.398	144.51329	0.00000	144.51318	395.72754	0.0000	-68.55812	0.32151	0.85020
10	1.20794	379.449	134.7374	0.00000	134.73743	402.69897	0.0000	-70.44526	0.29871	0.86491
11	1.24450	391.000	124.86534	0.00000	124.86534	410.45337	0.0000	-72.28892	0.26504	0.88123

Table 4-3

RESULTS FOR SPFL UNMODIFIED

PLANE NO. 1 VXR(1)= 164.0000

J	R	U	VX 2	VT 2	V 2	W 2	ALPHA 2	BETA 2	MV 2	MA 2
1	0.90700	284.942	164.00000	0.00000	164.00000	328.76758	0.00000	-60.0772	0.34102	0.68264
2	0.92756	291.401	164.00000	0.00000	164.00000	334.38037	0.00000	-61.6202	0.34102	0.69532
3	0.94785	297.775	164.00000	0.00000	164.00000	339.94995	0.00000	-61.1561	0.34102	0.70690
4	0.96805	304.121	164.00000	0.00000	164.00000	345.52148	0.00000	-61.6638	0.34102	0.71848
5	0.98833	310.493	164.00000	0.00000	164.00000	351.14429	0.00000	-62.1574	0.34102	0.73018
6	1.00866	316.842	164.00000	0.00000	164.00000	356.85889	0.00000	-62.6409	0.34102	0.74206
7	1.02970	323.516	164.00000	0.00000	164.00000	362.70996	0.00000	-63.1182	0.34102	0.75423
8	1.05128	330.270	164.00000	0.00000	164.00000	368.74658	0.00000	-63.5927	0.34102	0.76675
9	1.07352	337.256	164.00000	0.00000	164.00000	375.01636	0.00000	-64.0674	0.34102	0.77982
10	1.09668	344.533	164.00000	0.00000	164.00000	381.57422	0.00000	-64.5453	0.34102	0.79345
11	1.12097	352.164	164.00000	0.00000	164.00000	388.47900	0.00000	-65.0290	0.34102	0.80781

PLANE NO. 2 VXR(2)= 158.0000

J	R	U	VX 1	VT 1	V 1	W 1	ALPHA 1	BETA 1	MV 1	MA 1
1	0.90700	284.942	158.00000	427.45288	455.71024	212.77502	60.7141	42.0049	0.97566	0.44414
2	0.92681	294.308	158.00000	413.85083	442.98584	198.12756	69.1042	37.1117	0.94389	0.42216
3	0.94528	303.251	158.00000	401.64575	431.60547	186.13293	68.5263	31.9127	0.91529	0.39602
4	0.96284	311.909	158.00000	390.49409	421.24051	176.46484	67.9711	26.4450	0.88609	0.37494
5	1.01984	320.391	158.00000	380.15894	411.68330	168.92664	67.4314	20.7206	0.85775	0.35853
6	1.04654	328.785	158.00000	370.45264	402.73950	163.40173	66.9015	14.7735	0.85386	0.34643
7	1.07325	337.172	158.00000	361.23828	394.28052	159.82227	66.3762	8.6607	0.84110	0.33851
8	1.10015	345.622	158.00000	352.40649	386.20508	158.14551	65.8511	2.4588	0.841725	0.33445
9	1.12747	354.204	158.00000	343.85841	378.43042	158.33765	65.3223	-3.7425	0.84117	0.33477
10	1.15541	362.983	158.00000	335.55103	370.88892	162.36365	64.7858	-9.8494	0.78451	0.33877
11	1.18420	372.028	158.00000	327.32282	363.52466	164.18372	64.2380	-15.7751	0.74735	0.34657

PLANE NO. 3 VXR(3)= 164.0000

J	R	U	VX 2	VT 2	V 2	W 2	ALPHA 2	BETA 2	MV 2	MA 2
1	0.90700	284.942	164.00000	0.00000	164.00000	328.76758	0.00000	-60.0772	0.34570	0.70705
2	0.94114	295.668	164.00000	0.00000	164.00000	338.10547	0.00000	-60.984	0.34570	0.72713
3	0.97439	306.113	164.00000	0.00000	164.00000	347.27661	0.00000	-61.8198	0.34570	0.74686
4	1.00710	316.389	164.00000	0.00000	164.00000	356.36670	0.00000	-62.6091	0.34570	0.76641
5	1.03959	326.595	164.00000	0.00000	164.00000	365.45850	0.00000	-63.3365	0.34570	0.78596
6	1.07213	336.819	164.00000	0.00000	164.00000	374.62354	0.00000	-64.0382	0.34570	0.80567
7	1.10490	347.142	164.00000	0.00000	164.00000	383.93066	0.00000	-64.7126	0.34570	0.82565
8	1.13840	357.642	164.00000	0.00000	164.00000	393.45020	0.00000	-65.3658	0.34570	0.84614
9	1.17265	368.398	164.00000	0.00000	164.00000	403.25195	0.00000	-66.0020	0.34570	0.86724
10	1.20795	379.489	164.00000	0.00000	164.00000	413.41064	0.00000	-66.6279	0.34570	0.88919
11	1.24450	391.000	164.00000	0.00000	164.00000	424.00073	0.00000	-67.2450	0.34570	0.91184

Table 4-1

RESULTS FOR SRE MODIFIED BY FLARE, DISK

J	V1/V2	W2/W1	DALPHA	DBETA
1	2.43327	1.41665	65.18956	-91.48114
2	2.37983	1.53639	64.62851	-88.13623
3	2.35155	1.66258	64.31639	-85.13683
4	2.34477	1.79864	64.27928	-82.31281
5	2.35732	1.94801	64.46611	-79.49109
6	2.38911	2.11319	64.84843	-76.48756
7	2.43482	2.29491	65.47021	-73.11417
8	2.50201	2.49085	66.63732	-69.18687
9	2.59101	2.69364	66.91760	-64.54715
10	2.69691	2.88906	67.84023	-59.10245
11	2.82455	3.05579	68.84579	-52.48031

RESULTS FOR SRE, UNMODIFIED

J	V1/V2	W2/W1	DALPHA	DBETA
1	2.77978	1.54514	69.71412	-102.12654
2	2.70113	1.70652	69.13419	-98.19522
3	2.63174	1.86575	68.52631	-93.73242
4	2.56459	2.01948	67.97108	-89.34512
5	2.51028	2.16341	67.43144	-84.45712
6	2.45573	2.29265	66.90147	-78.41166
7	2.40415	2.40224	66.37621	-73.37326
8	2.35491	2.48790	65.85114	-67.42462
9	2.30750	2.54679	65.32228	-62.26025
10	2.26152	2.57706	64.78581	-56.77838
11	2.21461	2.58248	64.23804	-51.46938

Table L-5

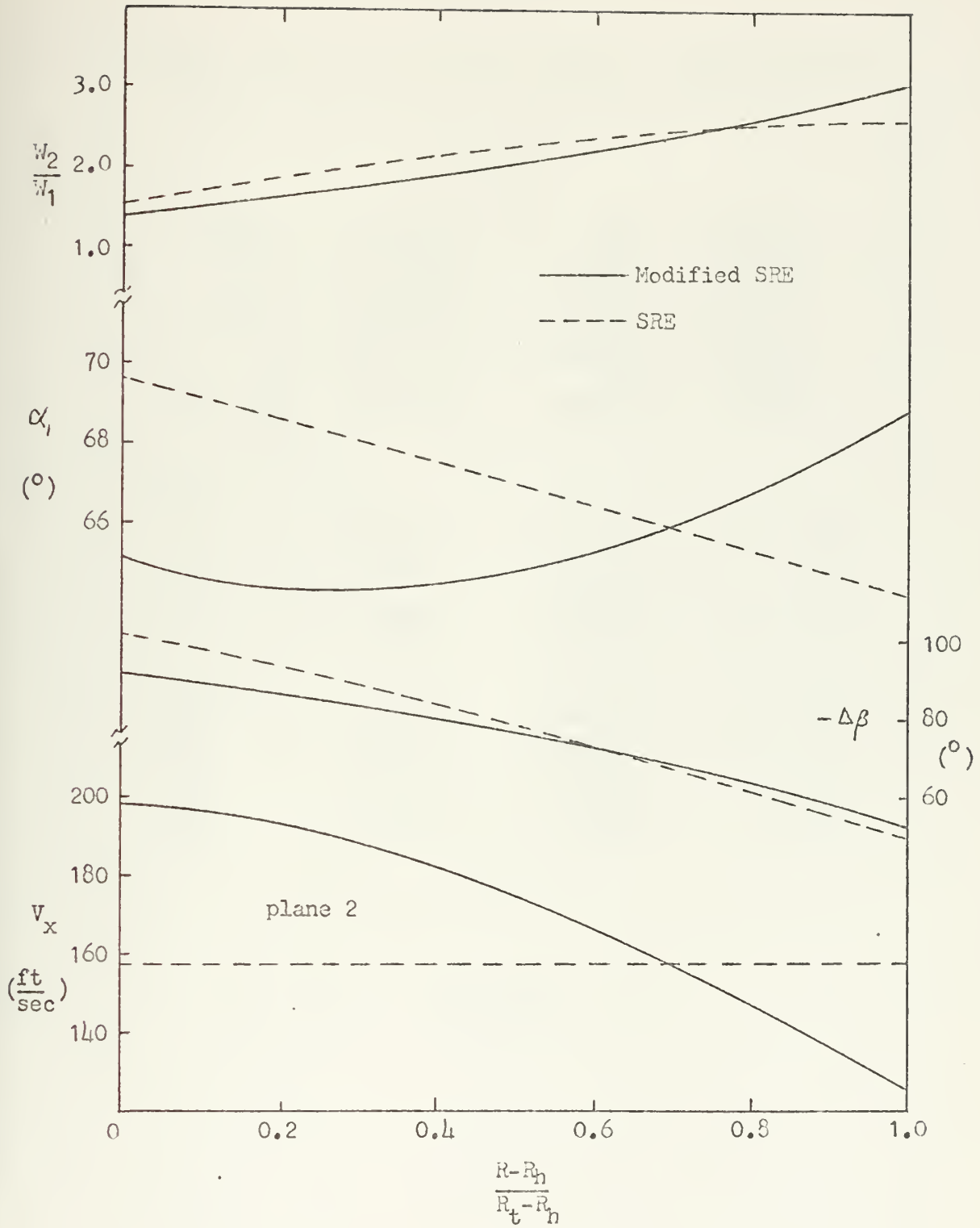


Figure 4-6

RUN NO. 12

SIMPLE RADIAL EQUILIBRIUM PRELIM TURBINE DESIGN
WITH FLARE AND ACTUATOR DISK CORRECTIONS

INPUTS

GAMMA=	1.1300	HS=	0.245000
PGAS=	10.9000	HR=	0.307000
RPM=	3000.000	TEST1=	0.002760
FLOW=	284.5000	TEST2=	0.001380
REF=	0.907000	TEST3=	0.000138
VE=	0.286482	TEST4=	0.000140
WS=	0.083000	WR=	0.083000
PHITIP=	36.7594	PHIHUB=	0.0000
JJ=	11		

PLANE	1	2	3
T0(I)	588.0000	588.0000	550.0000
P0(I)	60.0000	60.0000	33.6200
RT(I)	1.120999	1.183000	1.245000
R(I,1)	0.907000	0.907000	0.907000
R0(I)	0.907000	0.907000	0.907000
VX0(I)	164.0000	180.2300	158.9000
B(I)	0.00000	280.00000	-107.70000
A0(I)	0.00000	0.00000	0.00000
A1(I)	0.00000	47.20000	47.20000
A2(I)	0.00000	0.00000	0.00000

Table 4-7

RESULTS FOR SRE MODIFIED BY FLARE, DISK

PLANE NO. 1 VXR(1)= 107.4142

J	R	U	VX 2	VT 2	V 2	W 2	ALPHA 2	BETA 2	MV 2	W 2
1	0.00700	284.042	105.71303	0.01000	195.71307	345.68213	0.0000	-55.5164	0.47352	0.71097
2	0.02739	291.348	104.18707	0.02000	194.18707	350.13257	0.0000	-56.3153	0.47441	0.72014
3	0.04755	297.682	100.77735	0.03000	190.77734	353.56560	0.0000	-57.3452	0.47724	0.73621
4	0.06767	304.001	105.68623	0.04000	185.68665	356.22405	0.0000	-58.5431	0.48053	0.74153
5	0.08790	310.358	179.13559	0.05000	179.13550	358.34497	0.0000	-60.0049	0.48277	0.74565
6	1.00842	316.803	171.35114	0.06000	171.35107	361.17407	0.0000	-61.5021	0.48514	0.74921
7	1.02938	323.390	142.55926	0.07000	162.55957	361.94775	0.0000	-63.3125	0.48811	0.75254
8	1.05039	330.174	152.98722	0.08000	152.98709	363.88233	0.0000	-65.1401	0.49170	0.75631
9	1.07330	337.214	142.82211	0.09000	142.82202	366.21265	0.0000	-67.0456	0.49472	0.76041
10	1.09683	344.578	132.27702	0.10000	132.27771	369.00570	0.0000	-68.0091	0.49747	0.76440
11	1.12153	352.339	121.52354	0.11000	121.52354	372.70605	0.0000	-70.0705	0.49927	0.77360

PLANE NO. 2 VXR(2)= 187.1499

J	R	U	VX 1	VT 1	V 1	W 1	ALPHA 1	BETA 1	MV 1	W 1
1	0.00700	284.042	102.27048	351.52026	400.66772	203.47144	61.3228	19.0005	0.84026	0.43124
2	0.02739	293.427	189.34853	343.86865	392.55371	195.95215	61.1610	14.9171	0.83123	0.41495
3	0.04755	301.720	184.56914	336.87451	384.12200	187.88721	61.2823	10.7039	0.81065	0.39740
4	0.06767	309.916	178.19843	330.39575	375.38794	179.37134	61.6599	6.5564	0.79347	0.37911
5	1.01254	318.098	170.49929	324.32422	366.41016	170.61328	62.0688	2.0413	0.77368	0.36725
6	1.03870	326.344	161.72713	318.57593	357.27612	161.91345	62.8551	-2.7499	0.75367	0.34156
7	1.06548	334.729	152.12079	313.06325	348.08301	153.65308	64.0859	-8.0086	0.73353	0.32382
8	1.09287	343.333	141.90207	307.73028	338.92651	146.20564	65.2437	-14.0621	0.71365	0.30892
9	1.12121	352.239	131.27226	302.65112	329.89474	142.32568	66.5517	-21.0693	0.69423	0.29521
10	1.15080	361.535	120.41103	297.62598	321.06079	136.32027	67.9732	-27.0575	0.67448	0.28655
11	1.18197	371.326	109.47624	292.65164	312.48608	134.79626	69.4919	-35.0024	0.65493	0.28313

PLANE NO. 3 VXR(3)= 166.8169

J	R	U	VX 2	VT 2	V 2	W 2	ALPHA 2	BETA 2	MV 2	W 2
1	0.00700	284.042	105.33038	-75.93272	209.57031	410.34668	-21.2431	-61.5747	0.45196	0.82476
2	0.04143	295.757	104.41505	-69.96565	206.62207	414.18579	-10.7926	-62.0052	0.44147	0.80288
3	0.07485	306.258	101.30214	-64.40559	201.95728	417.21216	-18.6148	-62.6942	0.43124	0.80914
4	1.00766	316.566	106.55247	-59.31932	195.75659	419.63232	-17.6394	-63.6747	0.42172	0.80402
5	1.04020	326.787	100.18779	-54.44086	188.23242	421.66577	-16.8113	-64.7022	0.41233	0.80081
6	1.07275	337.013	172.57655	-49.76277	179.60779	423.53027	-16.0850	-65.9539	0.39458	0.91158
7	1.10559	347.332	143.98066	-45.22983	170.10376	425.43984	-15.4202	-67.3288	0.36504	0.91522
8	1.13900	357.828	154.63916	-40.79535	159.92960	427.56641	-14.7785	-68.7071	0.34284	0.91934
9	1.17325	368.589	144.76817	-36.41827	149.27856	430.11132	-14.1205	-70.3208	0.32182	0.92434
10	1.20863	379.702	134.55927	-32.06175	138.32617	433.19141	-13.4421	-71.0033	0.29714	0.93754
11	1.24544	391.265	124.17854	-27.60098	127.22893	436.07217	-12.5709	-73.4902	0.27312	0.93825

Table 4-8

RESULTS FOR SRE, UNMODIFIED

PLANE NO. 1 VXR(1)= 164.0000

J	R	U	VX 2	VT 2	V 2	W 2	ALPHA 2	BETA 2	MV 2	W 2
1	0.90700	284.942	144.00000	0.00000	164.00000	328.76758	0.00000	-60.0772	1.34102	0.68364
2	0.92739	291.348	144.00000	0.00000	164.00000	334.33466	0.00000	-61.6248	0.34102	0.60522
3	0.94755	297.682	144.00000	0.00000	164.00000	339.86965	0.00000	-61.1484	0.34102	0.70673
4	0.96767	304.001	144.00000	0.00000	164.00000	345.41675	0.00000	-61.6544	0.34102	0.71827
5	0.98790	310.358	144.00000	0.00000	164.00000	351.02368	0.00000	-62.1470	0.34102	0.72992
6	1.00842	316.803	144.00000	0.00000	164.00000	356.73535	0.00000	-62.6307	0.34102	0.74180
7	1.02938	323.350	144.00000	0.00000	164.00000	362.59692	0.00000	-63.1092	0.34102	0.75399
8	1.05098	330.174	144.00000	0.00000	164.00000	368.66040	0.00000	-63.5841	0.34102	0.76660
9	1.07339	337.214	144.00000	0.00000	164.00000	374.97449	0.00000	-64.0644	0.34102	0.77974
10	1.09682	344.578	144.00000	0.00000	164.00000	381.61548	0.00000	-64.5481	0.34102	0.79354
11	1.12153	352.339	144.00000	0.00000	164.00000	388.63599	0.00000	-65.0394	0.34102	0.80814

PLANE NO. 2 VXR(2)= 162.2300

J	R	U	VX 1	VT 1	V 1	W 1	ALPHA 1	BETA 1	MV 1	W 1
1	0.90700	284.942	180.22908	351.52026	395.03076	192.13403	62.8551	20.2745	1.52674	0.40694
2	0.92401	293.427	175.24329	342.84865	385.94800	182.35152	62.9956	16.0580	1.81164	0.38584
3	0.94041	301.720	170.33472	331.87451	377.48050	173.92456	63.1773	11.6413	0.73004	0.36764
4	0.95650	309.916	165.44002	320.30575	369.50244	166.74034	63.4013	7.0566	0.74447	0.35211
5	1.01254	318.098	160.50305	324.32422	361.86670	160.62366	63.6649	2.2214	0.74372	0.33907
6	1.03879	326.344	155.46204	314.57593	354.48438	155.45588	63.9881	-2.8664	0.74757	0.32826
7	1.06548	334.729	150.25623	313.08325	347.27222	151.80737	64.3625	-8.1978	0.73182	0.31991
8	1.09287	343.333	144.81689	307.79028	340.15608	149.11487	64.8028	-13.7598	0.71133	0.31402
9	1.12121	352.239	139.06344	302.64112	333.07104	147.63989	65.3220	-19.6253	0.70092	0.31072
10	1.15080	361.535	132.89807	297.62598	325.94971	147.46606	65.9379	-25.6824	0.68547	0.31012
11	1.18197	371.326	126.19502	292.64164	318.72876	148.69556	66.6757	-31.9310	0.66084	0.31254

PLANE NO. 3 VXR(3)= 158.9000

J	R	U	VX 2	VT 2	V 2	W 2	ALPHA 2	BETA 2	MV 2	W 2
1	0.90700	284.942	158.89990	-75.93272	176.11060	394.30008	-25.5415	-66.2352	0.37096	0.84853
2	0.94143	295.757	140.38440	-60.96565	174.98006	399.34399	-23.5646	-66.3206	0.37653	0.85932
3	0.97485	306.258	141.70003	-64.46559	174.07751	404.45312	-21.7357	-66.4343	0.37457	0.87027
4	1.00764	316.566	162.88104	-50.31032	173.34717	409.65820	-20.0109	-66.5715	0.37205	0.88143
5	1.04020	326.787	163.95064	-54.44086	172.75281	414.98682	-18.3691	-66.7204	0.37164	0.89287
6	1.07275	337.013	144.02371	-40.76277	172.26770	420.46097	-16.7972	-66.9063	0.37064	0.90465
7	1.10559	347.332	145.81306	-45.22083	171.87195	426.14404	-15.2576	-67.1013	0.36978	0.91684
8	1.13907	357.828	146.62988	-40.72035	171.55103	432.04761	-13.7569	-67.3145	0.36924	0.92952
9	1.17325	368.589	147.37708	-36.41827	171.29321	438.22876	-12.2752	-67.5462	0.36852	0.94281
10	1.20862	379.702	148.05869	-32.06175	171.08048	444.73828	-10.8029	-67.7075	0.36808	0.95684
11	1.24544	391.265	148.67484	-27.69098	170.93262	451.63647	-9.3230	-68.0694	0.36774	0.97163

Table 4-9

RESULTS FOR SRE MODIFIED BY FLARE, DISK

I	V1/V2	W2/W1	DALPHA	DELTA
1	2.04721	2.01672	61.32275	-82.67424
2	2.02151	2.11371	61.16101	-76.32229
3	2.01346	2.22055	61.22226	-73.47844
4	2.02162	2.33946	61.65988	-72.16464
5	2.04544	2.47147	62.26875	-66.79347
6	2.08525	2.61578	63.22512	-63.27464
7	2.14126	2.76882	64.22586	-59.23222
8	2.21549	2.92282	65.24869	-54.73514
9	2.30983	3.06502	66.55167	-49.63699
10	2.42717	3.17775	67.97316	-43.74576
11	2.57140	3.24172	69.49193	-37.79771

RESULTS FOR SRE, UNMODIFIED

I	V1/V2	W2/W1	DALPHA	DELTA
1	2.40172	2.05226	62.85566	-86.54077
2	2.35334	2.18988	62.99559	-82.37854
3	2.32177	2.32545	63.17734	-78.20557
4	2.25306	2.45741	63.40126	-73.62814
5	2.20450	2.58362	63.66992	-68.95285
6	2.16149	2.70128	63.98812	-64.44575
7	2.11751	2.80714	64.36250	-58.30356
8	2.07413	2.89741	64.82281	-53.02463
9	2.03192	2.96823	65.32106	-47.92193
10	1.98750	3.01587	65.93703	-42.11513
11	1.94347	3.03732	66.67570	-36.13893

Table 4-10

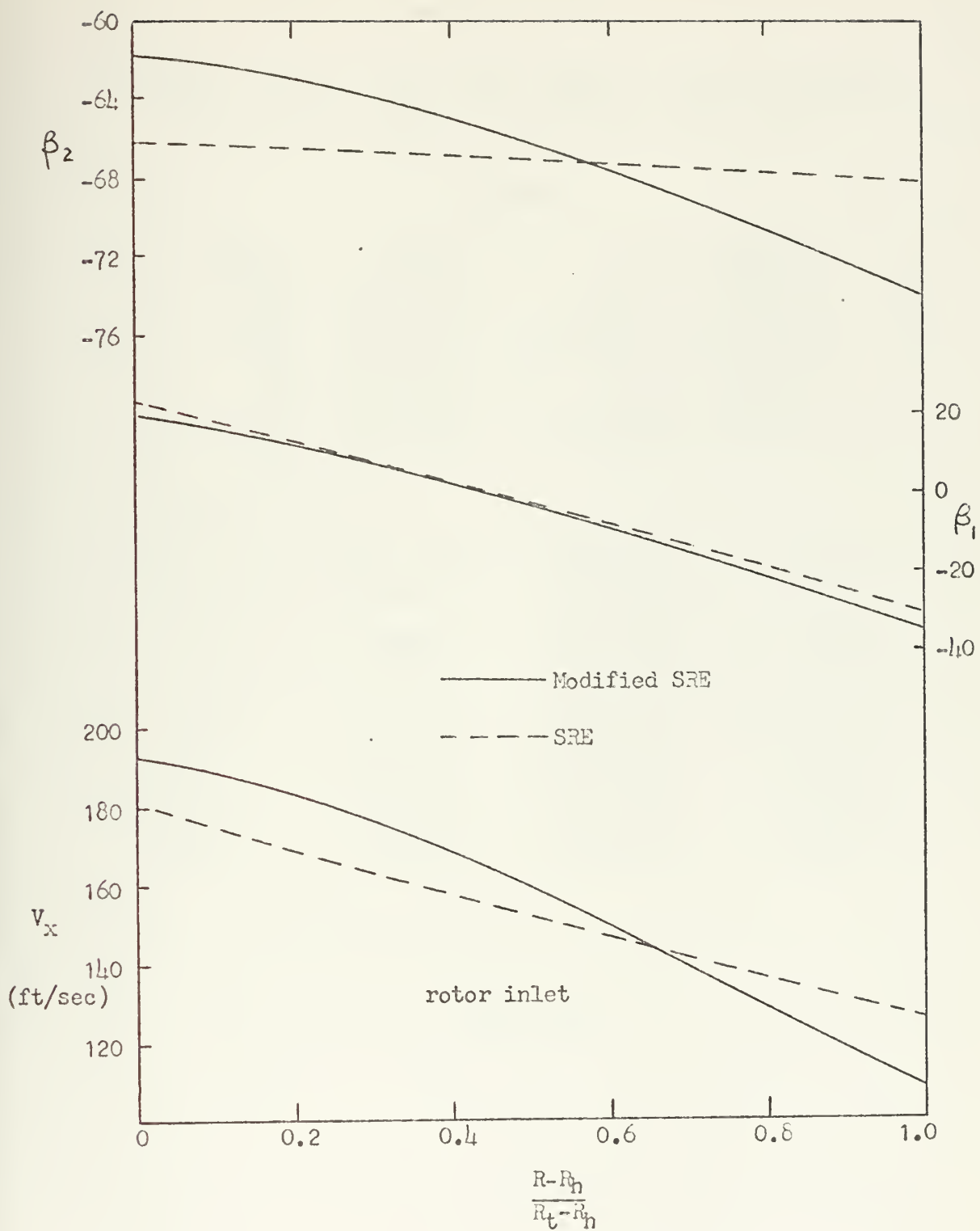


Figure 4-11

RUN NO. 2

SIMPLE RADIAL EQUILIBRIUM PRELIM TURBINE DESIGN
WITH FLARE AND ACTUATOR DISK CORRECTIONS

INPUTS

GAMMA=	1.1300	HS=	0.280000
RGAS=	10.9000	HR=	0.361541
RPM=	3910.000	TEST1=	0.003010
FLOW=	236.6000	TEST2=	0.001645
REF=	0.907000	TEST3=	0.000161
WE=	0.245925	TEST4=	0.000100
AS=	0.083000	WR=	0.283000
PHITIP=	26.0100	PHIHUB=	-26.0100
JJ=	11		

PLANE	1	2	3
T0(I)	588.0000	588.0000	552.0000
P0(I)	60.0000	60.0000	33.6000
RT(I)	1.026999	1.067500	1.138230
R(I,1)	0.787000	0.746500	0.726230
R0(I)	0.907000	0.907000	0.907000
VX0(I)	133.0000	214.0000	133.0000
B(I)	0.00000	505.19995	0.00000
A0(I)	0.00000	0.00000	0.00000
A1(I)	0.00000	0.00000	0.00000
A2(I)	0.00000	0.00000	0.00000

Table 4-12

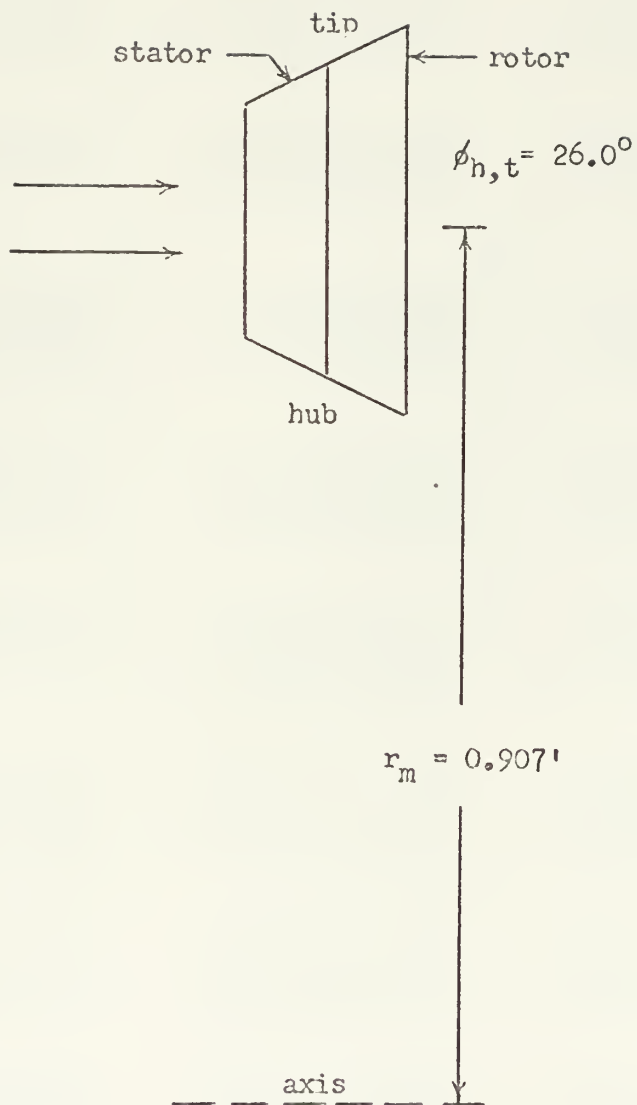


Figure 4-13

RESULTS FOR SRE MODIFIED BY FLARE, DISK

PLANE NO. 1 VXR(1)= 103.5471

J	R	U	VX 2	VT 2	V 2	W 2	ALPHA 2	BETA 2	MV 2	NU 2
1	0.78700	322.240	115.56578	0.00000	115.56578	342.33643	0.00000	-70.2705	0.23685	0.71051
2	0.81661	334.365	127.32050	0.00000	127.32050	357.78491	0.22000	-69.1541	0.26436	0.74287
3	0.84320	345.251	135.44820	0.00000	135.44820	370.87036	0.00000	-68.5791	0.28132	0.77027
4	0.86786	355.347	140.47069	0.00000	140.47069	382.10376	0.22000	-68.4328	0.29180	0.79375
5	0.89127	364.635	142.72847	0.00000	142.72847	391.85181	0.00000	-68.6393	0.29652	0.81408
6	0.91394	374.217	142.52147	0.00000	142.52147	402.43799	0.00000	-69.1505	0.29699	0.83191
7	0.93624	383.349	140.15057	0.00000	140.15057	409.16406	0.00000	-69.9179	0.29113	0.84786
8	0.95850	392.461	135.92725	0.00000	135.92725	415.33228	0.00000	-70.8967	0.28232	0.86263
9	0.98299	401.670	130.17278	0.00000	130.17278	422.23584	0.00000	-72.0436	0.27731	0.87678
10	1.00399	411.066	123.20920	0.00000	123.20920	429.15283	0.00000	-73.3157	0.25578	0.89092
11	1.02775	420.818	115.35045	0.00000	115.35045	436.33984	0.00000	-74.6712	0.23648	0.90566

PLANE NO. 2 VXR(2)= 397.8203

J	R	U	VX 1	VT 1	V 1	W 1	ALPHA 1	BETA 1	MV 1	NU 1
1	0.74650	305.657	185.25212	676.75830	731.65527	414.77002	74.6912	63.4718	1.56498	0.92511
2	0.80036	327.707	206.28498	631.22314	664.07520	366.98120	71.9025	55.7981	1.44602	0.81181
3	0.84243	344.935	219.50521	599.69629	638.80645	336.28823	69.8960	49.2515	1.44428	0.74000
4	0.87814	359.559	226.74506	575.31566	618.37646	312.98560	68.4892	43.5762	1.35535	0.68607
5	0.90994	372.577	229.16704	555.20288	600.63916	293.03491	67.5710	38.5517	1.31206	0.64011
6	0.93915	384.540	227.67407	537.93188	584.12842	274.52612	67.0600	33.9696	1.27213	0.59787
7	0.96662	395.788	223.02704	522.04380	568.24072	256.58032	66.8907	29.6308	1.23408	0.55722
8	0.99293	406.558	215.88727	508.79785	552.70459	238.87292	67.0081	25.3412	1.19713	0.51739
9	1.01849	417.026	206.82922	496.02661	537.42041	221.40320	67.3652	20.9048	1.16108	0.47833
10	1.04366	427.331	196.35103	484.06519	522.37207	204.38306	67.9211	16.1162	1.12684	0.44050
11	1.06872	437.592	184.87927	472.71460	507.58203	188.18591	68.6395	10.7567	1.09146	0.40466

PLANE NO. 3 VXR(3)= 98.4891

J	R	U	VX 2	VT 2	V 2	W 2	ALPHA 2	BETA 2	MV 2	NU 2
1	0.70600	289.074	116.39807	0.00000	116.39807	311.62517	0.00000	-68.0675	0.24983	0.66885
2	0.75976	311.084	128.79903	0.00000	128.79905	336.69312	0.00000	-67.5089	0.27457	0.72298
3	0.80643	330.197	137.06703	0.00000	137.06787	357.51514	0.00000	-67.4562	0.28442	0.76794
4	0.84870	347.502	141.04054	0.00000	141.94043	375.37329	0.00000	-67.7882	0.30495	0.80647
5	0.88810	363.635	143.91011	0.00000	143.91003	391.07642	0.00000	-68.4087	0.32021	0.84727
6	0.92566	379.013	143.30308	0.00000	143.39307	405.23071	0.00000	-69.2767	0.33809	0.87467
7	0.96218	393.936	140.77647	0.00000	140.77661	418.33276	0.00000	-70.3352	0.35243	0.89872
8	0.99800	408.635	136.43005	0.00000	136.43005	430.80786	0.00000	-71.5975	0.29304	0.92535
9	1.03383	423.304	130.70270	0.00000	130.70244	443.02246	0.00000	-72.8410	0.28363	0.95137
10	1.06990	438.111	123.92043	0.00000	123.92044	455.29761	0.00000	-74.2063	0.26104	0.97747
11	1.10687	453.212	116.38016	0.00000	116.38016	467.91406	0.00000	-75.5982	0.24079	1.00429

Table 4-14

RESULTS FOR SPE, UNMODIFIED

PLANE NO. 1 VXRI 1) = 133.0000

J	R	U	VX 2	VT 2	V 2	W 2	ALPHA 2	BETA 2	MV 2	1% 2
1	0.78700	322.240	133.00000	0.00000	133.00000	342.60840	0.00000	-67.5723	0.27621	0.72337
2	0.81661	334.365	133.00000	0.00000	133.00000	359.84521	0.00000	-68.3080	0.27621	0.74731
3	0.84320	345.251	133.00000	0.00000	133.00000	369.98340	0.00000	-68.9321	0.27621	0.76836
4	0.86786	355.347	133.00000	0.00000	133.00000	379.42090	0.00000	-69.4800	0.27621	0.78796
5	0.89127	364.635	133.00000	0.00000	133.00000	388.41406	0.00000	-69.9754	0.27621	0.80663
6	0.91391	374.217	133.00000	0.00000	133.00000	397.14868	0.00000	-70.4344	0.27621	0.82477
7	0.93624	383.349	133.00000	0.00000	133.00000	405.76465	0.00000	-70.8662	0.27621	0.84264
8	0.95850	392.461	133.00000	0.00000	133.00000	414.38354	0.00000	-71.2792	0.27621	0.86056
9	0.98099	401.670	133.00000	0.00000	133.00000	423.11621	0.00000	-71.6784	0.27621	0.87817
10	1.00390	411.086	133.00000	0.00000	133.00000	432.06567	0.00000	-72.0719	0.27621	0.89728
11	1.02774	420.818	133.00000	0.00000	133.00000	441.33398	0.00000	-72.4604	0.27621	0.91653

PLANE NO. 2 VXRI 2) = 214.0000

J	R	U	VX 1	VT 1	V 1	W 1	ALPHA 1	BETA 1	MV 1	1% 1
1	0.74650	305.657	214.00000	676.75830	709.78711	428.38281	72.4524	60.0204	1.58456	0.95724
2	0.80035	327.707	214.00000	631.22314	666.51221	371.37305	71.2721	54.8135	1.47517	0.82195
3	0.84243	344.935	214.00000	599.69429	636.73486	332.71484	70.3612	49.9697	1.40063	0.73182
4	0.87814	359.559	214.00000	575.31566	613.81787	303.87939	69.5960	45.2329	1.34414	0.66544
5	0.90994	372.577	214.00000	555.20288	595.01758	281.32252	68.9211	40.4771	1.29342	0.61391
6	0.93915	384.540	214.00000	537.93188	578.93555	263.29663	68.3064	35.6324	1.25065	0.57284
7	0.96662	395.788	214.00000	522.64380	564.75879	248.77393	67.7331	30.6584	1.22575	0.53934
8	0.99293	406.558	214.00000	508.79785	551.97021	237.16858	67.1845	25.5363	1.19538	0.51363
9	1.01849	417.026	214.00000	494.02661	540.22021	228.11633	66.6633	22.2622	1.16765	0.49376
10	1.04366	427.331	214.00000	484.04519	529.25879	221.39270	66.1503	14.8483	1.14194	0.47760
11	1.06875	437.592	214.00000	472.71460	518.89746	216.86304	65.6436	9.3206	1.11774	0.46714

PLANE NO. 3 VXRI 3) = 133.0000

J	R	U	VX 2	VT 2	V 2	W 2	ALPHA 2	BETA 2	MV 2	1% 2
1	0.70600	289.074	133.00000	0.00000	133.00000	318.20215	0.00000	-65.2934	0.24464	0.64338
2	0.75975	311.084	133.00000	0.00000	133.00000	338.32231	0.00000	-66.8515	0.24464	0.72661
3	0.80643	330.197	133.00000	0.00000	133.00000	355.97534	0.00000	-68.0610	0.24464	0.74451
4	0.84870	347.502	133.00000	0.00000	133.00000	372.08472	0.00000	-69.0566	0.24464	0.79311
5	0.88810	363.635	133.00000	0.00000	133.00000	387.19458	0.00000	-69.9110	0.24464	0.83154
6	0.92566	379.013	133.00000	0.00000	133.00000	401.67058	0.00000	-70.6634	0.24464	0.86265
7	0.96210	393.936	133.00000	0.00000	133.00000	415.78827	0.00000	-71.3444	0.24464	0.89295
8	0.99800	408.435	133.00000	0.00000	133.00000	429.73389	0.00000	-71.9713	0.24464	0.92291
9	1.03383	423.304	133.00000	0.00000	133.00000	443.70557	0.00000	-72.5576	0.24464	0.95202
10	1.06990	438.111	133.00000	0.00000	133.00000	457.85220	0.00000	-73.1130	0.24464	0.98331
11	1.10687	453.212	133.00000	0.00000	133.00000	472.32202	0.00000	-73.6451	0.24464	1.01438

Table 4-15

RESULTS FOR SRE MODIFIED BY FLARE, DISK

J	V1/V2	W2/W1	DALPHA	DRF TA
1	6.07148	2.75133	74.63122	-131.53932
2	5.21578	2.91747	71.90254	-123.30499
3	4.71477	1.06314	69.89600	-116.70772
4	4.40218	1.19953	68.48915	-111.35825
5	4.20827	1.33457	67.57100	-106.96034
6	4.09453	1.47611	67.06060	-103.24632
7	4.05450	1.63042	66.89072	-99.96630
8	4.06518	1.80350	67.03869	-96.57872
9	4.12852	2.00008	67.36522	-93.74585
10	4.22971	2.22767	67.92110	-90.32257
11	4.40435	2.48645	68.63947	-86.35492

RESULTS FOR SRE, UNMODIFIED

J	V1/V2	W2/W1	DALPHA	DRF TA
1	5.33675	2.74282	72.45241	-125.32298
2	5.01137	2.91102	71.27214	-121.66501
3	4.78748	1.06901	70.36122	-118.43069
4	4.61517	1.22445	69.59602	-114.28949
5	4.47382	1.37629	68.92114	-110.38710
6	4.35290	1.52554	68.30637	-106.29588
7	4.24631	1.67132	67.73306	-102.00319
8	4.15215	1.81103	67.18846	-97.50761
9	4.06181	1.94508	66.66337	-92.81976
10	3.97939	2.06806	66.15033	-87.96123
11	3.90149	2.17797	65.64359	-82.96570

Table 4-16

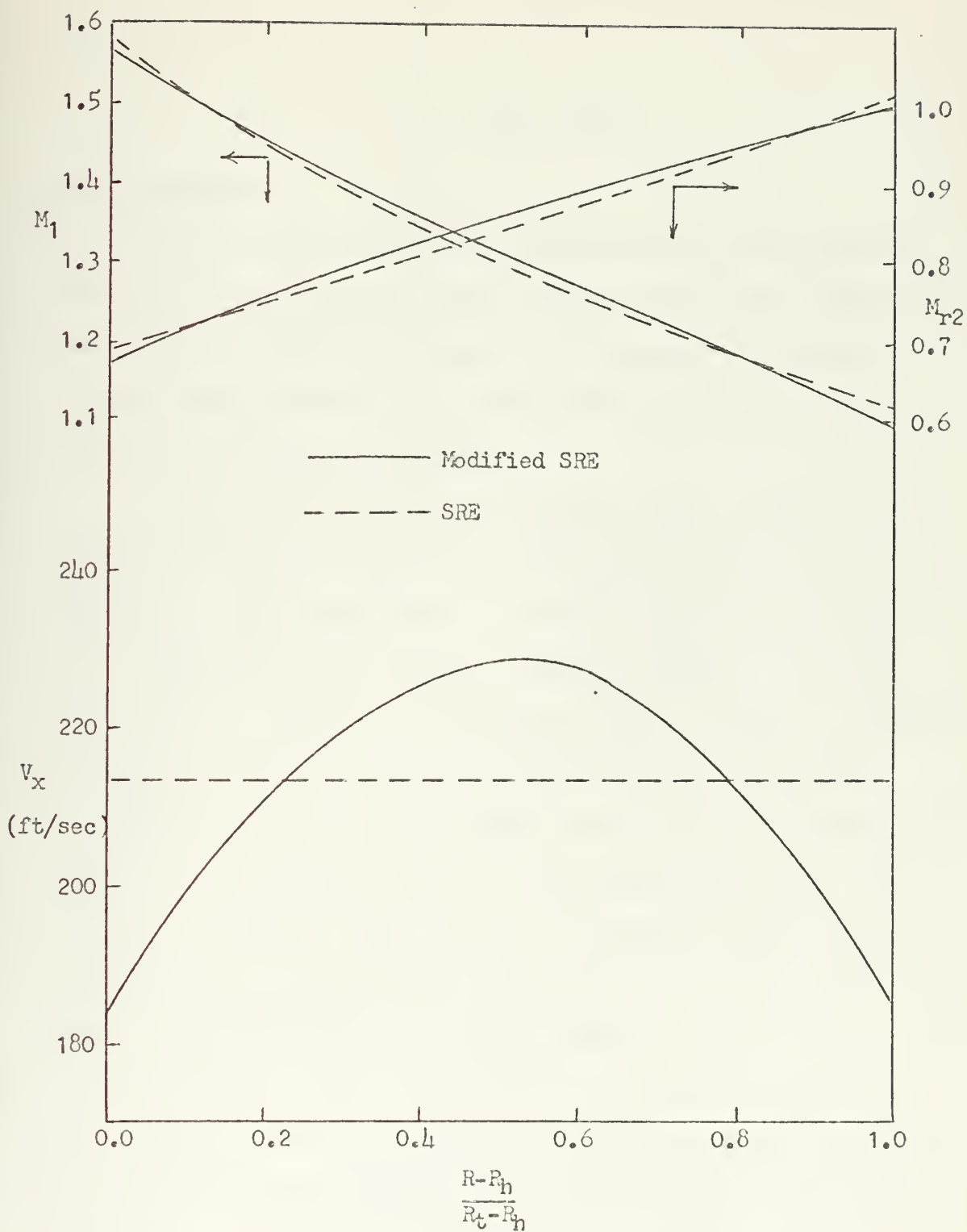


Figure 4-17

5. CONCLUSIONS

5.1 General

A model for improving a simple radial equilibrium design by modifying the axial velocity has been discussed. The computer program presented here provides a means to quickly and inexpensively incorporate the model into preliminary design procedure.

The improved preliminary design model is basically a perturbation of the simple radial equilibrium design procedure, and comparisons of the two procedures can be made easily from the computer program output. It would be useful to compare the improved model results to designs produced by more rigorous and complicated analytical procedures as well, to see where the balance of complexity versus accuracy lies. Since the program described here is only a "design tool" and was not derived analytically, comparisons to more exact procedures are really needed to give full respectability to the results.

The changes made as a result of applying the model to a simple radial equilibrium preliminary design are of a magnitude which suggests that they may have measurable effects upon turbine performance. Further study is needed to quantify these effects in terms of efficiencies.

5.2 Improving the Model

Aside from possible improvements in the generation of the correction to the simple radial equilibrium axial velocity, other changes in the program to extend its usefulness may be desirable. An example is extending the range of the program to include more than one stage, with two conical sections per stage.

5.3 Applications

The most direct application for the program is to refine the blade shapes of an axial turbine in preliminary design. However, less specific applications to research type problems may be fruitful. Used in conjunction with a sufficiently general simple radial equilibrium preliminary axial turbine design program, the program presented in this thesis could be used to generate a series of modified designs to explore the ramifications of flare and actuator disk effects. Perhaps it is possible to find a simple radial equilibrium tangential velocity distribution which will be less effected by the modification, or will "compensate" for the effects.

REFERENCES

1. Carmichael, A. Douglas, *Gas Turbine Engineering Handbook* (John W. Sawyer: Editor), Chapter 3, Gas Turbine Publications, Stamford, Connecticut, 1966.
2. Carmichael, A.D. and Pai, B.R., *Fluid Flow in Highly Flared Axial-Flow Turbines*, Imperial College of Science and Technology, Department of Mechanical Engineering, London, June 1968.
3. Horlock, J.H., *Axial Flow Compressors*, Butterworths Scientific Publications, London, 1958, Chapter 1.
4. Carmichael, A. Douglas, MIT Subject 13.26 Notes, unpublished, 1974.
5. Cravalho, Ernest G. and Smith, Joseph L., Jr., *Thermodynamics (An Introduction)*, Holt, Rinehart and Winston, Inc., 1971, Chapter 11.
6. Horlock, *Ibid.*, Chapter 5.
7. *IBM System/360 and System/370 FORTRAN IV Language*, IBM, 1974.
8. Cress, Paul, *FORTRAN IV With WATFOR And WATFIV*, Prentice-Hall, 1970.
9. MIT Subject 13.26 Design Project, Spring 1974.

APPENDIX A

Variable List

The following is an alphabetical list of variables which appear in the computer main program and subprograms.

The units are the same as those listed in the Notation section. The same variable names are used to represent identical quantities in both the main and subprograms. In addition, the subscripts are used in consistent manner throughout. An intermediate variable is one used locally in the program to simplify arithmetic expressions. Zero is written \emptyset . Unless otherwise indicated, variable naming follows the implicit REAL/INTEGER typing convention.

AREA	annulus area between two adjacent streamlines
$A\emptyset(I)$	constant term in the expression for tangential velocity
$A1(I)$	coefficient of r in the expression for tangential velocity
$A2(I)$	coefficient of r^2 in the expression for tangential velocity
$B(I)$	coefficient of $1/r$ in the expression for tangential velocity
C1	intermediate gas property constant used by RNEXT
C2	intermediate variable
C3	intermediate variable

D	intermediate variable
DALPHA	stator tuning angle
DBETA	rotor turning angle
DD(I,J)	actuator disk correction factor
DISK(I)	function subprogram which calculates the non-dimensional actuator disk correction factor
DM	mass flow per channel between streamlines
DR	difference between the calculated and actual tip radius
DROLD	value of DR in last iteration
DRZ	difference between R(I,J+1) and RGUESS calculated by STREAM
DRZOLD	value of DRZ in last iteration
F(I,1)	total absolute gas velocity
F(I,2)	total relative gas velocity
F(I,3)	alpha; absolute flow angle
F(I,4)	beta; relative flow angle
FF(I,J)	flare correction factor
FLARE(I)	function subprogram which calculates the non-dimensional flare correction factor
FLOW	total turbine mass flow
FVT(I)	function subprogram which calculates tangential velocity as a function of radius
FVX(I)	function subprogram which calculates axial velocity as a simple radial equilibrium function of radius
G	$g_0 = 32.1740 \text{ ft-lbm/lbf/sec}^2$
GAMMA	γ = ratio of specific heats; input constant

HR	mean rotor height
HS	mean stator height
I	subscript which identifies a transverse station along the turbine axis
	I = 1 stator leading edge I = 2 rotor leading edge I = 3 rotor trailing edge
ID	user determined input data identification number
IREAD	input device channel number
IWRITE	output device channel number
J	streamline index; J = 1,2,3, ..., JJ, starting at the hub
JJ	quantity of streamlines considered
JM1	quantity of flow channels considered
K	key variable; K = 1 modified simple radial equili- brium data K = 2 SRE data
KK	key variable; KK \neq 1 program diagnostics not printed KK = 1 diagnostics printed
L1	loop count; number of times all the streamlines for the turbine are calculated
L2	loop count; number of times a set of streamlines must be calculated at a station to satisfy the geometry
L3	loop count; the total number of times, during the calculation of a set of streamlines at a plane, that the subprogram RNEXT is called
MM	key used in labeling output data
MV	absolute mach number (REAL variable)

MW	relative mach number (REAL variable)
PHIHUB	hub flare angle
PHITIP	tip flare angle
N1	test variable for L1 loop divergence check
N2	test variable for L2 loop divergence check
N3	test variable for L3 loop divergence check
PI	3.14159
PØ(I)	stagnation pressure
R(I,J)	radial location of a streamline
REF	reference radius for flare correction
RGAS	specific gas constant; input data
RGUESS	temporary storage for a trial R(I,J+1)
RHO	static density
RNEXT(I)	function subprogram which calculates a trial value of R(I,J+1)
RPM	turbine rpm; input data
RR	intermediate variable used as the argument for FLARE(I), FVX(I), FVT(I)
RT(I)	tip radius
RØ(I)	input reference radius at which VX(I,J)=VXØ(I)
S	sum which accumulates the difference between streamline positions on the current iteration (L1) and the previous (L1-1)
SOLD	value of S from previous iteration
S1	term in S
TEST1	test value to terminate loop L1

TEST2	test value to terminate loop L2
TEST3	test value to terminate loop L3
TEST4	test value to ensure the axial velocity is positive
TGNT	tangent of the flare angle θ
TR	ratio of static to total temperature
T θ (I)	stagnation temperature
T1	input percent used to calculate TEST1
T2	input percent used to calculate TEST2
T3	input percent used to calculate TEST3
U	blade speed
VRATIO	V_1/V_2
VT(I,J)	tangential velocity
VTZ	average value of tangential velocity between two streamlines
VX(I,J)	axial velocity
VXR(I)	reference value of axial velocity; input data
VXSRE(I,J)	simple radial equilibrium axial velocity
VXZ	average value of axial velocity between two streamlines
VX θ (I)	input reference value of axial velocity
WE	entrance width dimension used to find the flare correction factor
WR	rotor width
WRATIO	W_2/W_1
WS	stator width
Z	intermediate variable
Z1, ..., Z6	intermediate variables

APPENDIX B

Program Listing

This appendix contains the computer program listing of the MAIN program, subroutine STREAM, and function subprograms RNEXT, FLARE, DISK, FVX, and FVT. Refer to the table below. The purpose of each program segment is indicated; flow charts for MAIN, STREAM, and RNEXT appear in Chapter 3.

<u>paragraph</u>	<u>segment</u>	<u>page</u>
B.1	MAIN	95
B.2	STREAM	103
B.3	functions	106

B.1 MAIN

The MAIN program reads the input data, governs the iteration loops to generate the streamlines, calculates the velocity triangles, and prints out the results. The listing begins on the next page.


```

C MAIN PROGRAM--APPLIES FLARE AND ACTUATOR DISK CORRECTIONS TO A PROFILE
C DESIGN BASED UPON SIMPLE RADIAL EQUILIBRIUM
  REAL R(3,11),VX(3,11),VT(3,11),VRATIO(11),PRATIO(11),DALPHA(11)
  REAL DETA(11)
  REAL MV,MW
  COMMON A2(3),A1(3),A2(3),R(3),C1,DN, F(3,4),
  GAMMA,G,HR,HS,IWRITE,IREAD, J,JJ,JM1,K,L1,L2,L3,PI,P2(3),Rn(3),
  R,RT(3),RPM,REF,RGAS, TW(3),TEST1,TEST2,TEST3,TEST4,VX,VT,
  VXR(3),VXZ(3),WE,WS,WR,VXZ,VTZ
  4,FF(3,11),DD(3,11),VXSRE(3,11)
C INSERT THE PROPER I/O CHANNEL NUMBERS
  IREAD= R
  IWRITE=5
  1 READ(IREAD,100)JJ,KK,IN
  READ(IREAD,110)GAMMA,RGAS
  READ(IREAD,120)RPM,FLOW,(TW(1),P0(I),I=1,3)
  READ(IREAD,130)R(1,1),FT(1),R(3,1),RT(3),WS,WR
  READ(IREAD,140)T1,T2,T3,TEST4
  READ(IREAD,150)(R0(I),VX0(I),I=1,3)
  READ(IREAD,160)(B(I),A0(I),A1(I),A2(I),I=1,3)
C BLANK CARD MUST FOLLOW EACH SET OF 7 INPUT DATA CARDS
  C2=R(3,1)-R(1,1)
  C3=RT(3)-RT(1)
C TEST FOR SINGULAR FLARE GEOMETRY
  IF(ABS(C3).GE.TEST4)GO TO 3
  IF(ABS(C2).GE.TEST4)GO TO 3
  WRITE(IWRITE,205)
  GO TO 45
C CALCULATE FLARE PARAMETERS, PLANE TWO HUR AND TIP RADII, AND BLADE HEIGHTS
  3 WE=(WR+WS)*(FT(1)-R(1,1))/(C3-C2)
  REF=R(1,1)-C2*WE/(WS+WR)
  RT(2)=(WR*RT(1)+WS*RT(3))/(WS+WR)
  R(2,1)=(WR*R(1,1)+WS*R(3,1))/(WS+WR)

```



```

PHITIP=57.29578*ATAN((RT(1)-REF)/WE)
PHIHUR=57.29578*ATAN((R(1,1)-PEF)/WE)
WR=(RT(2)-R(2,1)+RT(3)-R(3,1))/2.
HS=(RT(1)-R(1,1)+RT(2)-R(2,1))/2.
JM1=JJ-1
TEST1=T1*(RT(2)-R(2,1))
TEST2=T2*(RT(2)-R(2,1))
TEST3=T3*(RT(2)-R(2,1))/FLOAT(JM1)

C WRITE INPUT DATA
  WRITE(IWRITE,209)ID
  WRITE(IWRITE,210)GAMMA,HS,FGAS,HR,RPM,TEST1,FLOW,TEST2,REF,TEST3,
  & WE,TEST4,WS,UR,PHITIP,PHIHUR,JJ
  WRITE(IWRITE,211)((T0(I),I=1,3),(P0(I),I=1,3),(RT(I),I=1,3),(R(1,1)
  & ,I=1,3),(R0(I),I=1,3),(VX0(I),I=1,3),(B(I),I=1,3),(AP(I),I=1,3),(A2
  & P1(I),I=1,3),(A2(I),I=1,3)
  DO 4 I=1,3
    4 VXR(I)=VX0(I)
    G=32.1740
    C1=(GAMMA-1.)/(GAMMA*2.*G*FGAS)
    DN=FLOW/FLOAT(JM1)
    PI=3.14159
    IF(KK.EQ.1)WRITE(IWRITE,215)
    L1=1
    SOL0=RT(3)
    N1=0
    C THE LOOP THRU STATEMENT 20 CALCULATES STREAMLINE POSITIONS AND THE VELOCITIES
    C WHICH SATISFY THE GEOMETRY CONSTRAINT
      5 DO 20 I=1,3
        L2=1
        L3=0
        DR=RT(I)
        N2=0
        7 RR=R(I,1)

```



```

DROLDF=DR
VX(I,1)=FVX(I)
VXSRE(I,1)=VX(I,1)
VX(I,1)=VX(I,1)*FLARE(I)
FF(I,1)=FLARE(I)
VT(I,1)=FVT(I)
IF(L1.EQ.1)GO TO 10
J=0
DO(I,1)=DISK(I)
VX(I,1)=VX(I,1)*DISK(I)
10 S=0
C THE LOOP THRU STATEMENT 15 CALCULATES A TRIAL SET OF STREAMLINE POSITIONS FOR
C A PLANE
DO 15 J=1,JM1
IF(L1.EQ.1)R(I,J+1)=R(I,J)
S1=R(I,J+1)
CALL STRFAM(I)
IF(I.EQ.5)GO TO 45
S=S+ ABS(R(I,J+1)-S1)
15 CONTINUE
C TEST FOR THE GEOMETRY
DR=R(I,JJ)-RT(I)
IF(ABS(DR).LE.TEST2)GO TO 20
C WRITE PROGRAM DIAGNOSTIC DATA IF KK=1
IF(KK.EQ.1)WRITE(IWRITE,411)L2,VXR(I),VX(I,JJ),DR,R(I,JJ)
C CHECK FOR DIVERGENCE OF ITERATION PROCESS
IF(ABS(DR).GE.ABS(DROLDF))N2=N2+1
IF(N2.LT.2)GO TO 18
WRITE(IWRITE,215)I,L2,L3
GO TO 45
18 CONTINUE
C MODIFY THE REFERENCE VX USED BY FVX
VXP(I)=VXR(I)+ 2.*VX(I,JJ)*DR/(RT(I)-R(I,1))

```



```

L2=L2+1
GO TO 7
C WRITE PROGRAM DIAGNOSTIC DATA IF KK=1
  20 IF(KK.EQ.1)WRITE(IWRITE,220)L1,I,L2,L3,S,DR,VXR(I)
  IF(L1.EQ.1)GO TO 25
C IF STREAMLINE LOCATIONS HAVE NOT CHANGED MUCH, STOP ITERATING AND PROCEED
  IF(S.LE.TEST1)GO TO 30
C TEST FOR CONVERGENCE OF LOOP L1
  IF(1.NE.3)GO TO 25
  IF(S.OF.SOLD)N1=N1+1
  IF(N1.LT.2)GO TO 25
  WRITE(IWRITE,225)
  GO TO 45
C GO BACK AND RECALCULATE FOR ALL PLANES
  25 L1=L1+1
  GO TO 5
  30 DO 40 K=1,2
C CALCULATE VELOCITY TRIANGLE DATA AND PRINT RESULTS
C RESULTS FOR K=1 ARE SRE VALUES CORRECTED FOR FLARE AND ACTUATOR DISK
C RESULTS FOR K=2 ARE SRE VALUES
  IF(K.EQ.1)WRITE(IWRITE,231)
  IF(K.NE.1)WRITE(IWRITE,232)
  DO 35 I=1,3
  IF(K.EQ.2)VXP(I)=VX0(I)
  MM=2
  IF(1.EQ.2)MM=1
  WRITE(IWRITE,242)I,I,VXR(I),MM,MM,MM,MM,MM,MM,MM,MM
  DO 35 J=1,JJ
  U=2.*PI*RR*MM*(I,J)/60.
  IF(K.EQ.1)GO TO 32
  RR=R(I,J)
  VX(I,J)=FVX(I)
  VT(I,J)=FVT(I)

```



```

32 CONTINUE
C F(I,1) IS V
F(I,1)=SQRT(VT(I,J)*VT(I,J)+VX(I,J)*VX(I,J))
C VRATIO IS V1(PLANE 2) DIVIDED BY V2(PLANE 1)
IF(I.EC.1)VRATIO(J)=1./F(I,1)
IF(I.EC.2)VRATIO(J)=VRATIO(J)*F(2,1)
C F(I,2) IS W
F(I,2)=SQRT(VX(I,J)*VX(I,J)+(U-VT(I,J))**2)
C WRATIO IS W2(PLANE 3) DIVIDED BY W1(PLANE 2)
IF(I.EC.2)WRATIO(J)=1./F(2,2)
IF(I.EC.3)WRATIO(J)=WRATIO(J)*F(3,2)
C F(I,3) IS ALPHA
F(I,3)=ATAN(VT(I,J)/VX(I,J))*57.29578
C DALPHA IS THE STATOR TURNING ANGLE
IF(I.EC.1)DALPHA(J)=-F(1,3)
IF(I.EC.2)DALPHA(J)=DALPHA(J)+F(2,3)
C F(I,4) IS BETA
F(I,4)=ATAN((VT(I,J)-U)/VX(I,J))*57.29578
C DBETA IS THE ROTOR TURNING ANGLE
IF(I.EC.2)DBETA(J)=-F(2,4)
IF(I.EC.3)DBETA(J)=DBETA(J)+F(3,4)
MV=SQRT(1./(GAMMA*G*RGAS*(T0(I)/F(I,1)**2-C1)))
MW=MV*F(I,2)/F(I,1)
IF(KK.NE.1)GO TO 35
C WRITE PROGRAM DIAGNOSTIC DATA IF KK=1
IF(K.EC.1)WRITE(IWRITE,252)FF(I,J),DD(I,J),VXSRE(I,J)
35 WRITE(IWRITE,250)U,R(I,J),U,VX(I,J),VT(I,J),(F(I,M),M=1,4),MV,MW
IF(K.EC.1)WRITE(IWRITE,231)
IF(K.NE.1)WRITE(IWRITE,232)
WRITE(IWRITE,222)
DO 40 J=1,JJ
40 WRITE(IWRITE,270)J,VRATIO(J),WRATIO(J),DALPHA(J),DBETA(J)
45 GO TO 1

```



```

STOP
100 FORMAT(3I4)
110 FORMAT(2F10.4)
120 FORMAT(8F9.3)
130 FORMAT(6F10.6)
140 FORMAT(4F10.6)
150 FORMAT(6F10.6)
160 FORMAT(3(4F10.5,/))
205 FORMAT(25X,'NO FLARE IN THIS DESIGN')
209 FORMAT('I',55X,'RUN NO.',I4/)
210 FORMAT('O',38X,'SIMPLE RADIAL EQUILIBRIUM PRELIM TURBINE DESIGN',/
  1,42X,'WITH FLARE AND ACTUATOR DISK CORRECTIONS'//59X,'INPUTS'//43
  2X,'GAMMA=',F10.4,10X,'RS=',F10.6/44X,'RGAS=',F10.4,10X,'WR=',F10.6
  2/45X,'RPM=',F10.3,7X,'TEST1=',F10.6/44X,'FLOW=',F10.4,7X,'IFST2=',
  4F10.6/45X,'REF=',F10.6,7X,'TEST3=',F10.6/46X,'WE=',F10.6,7X,'TEST4
  5=',F10.6/46X,'RS=',F10.6,10X,'WR=',F10.6/42X,'PHITIP=',F10.4,6X,'D
  6H HUB=',F10.4/46X,'JJ=',I4)
211 FORMAT('O',39X,'PLANE',I9X,'I',12X,'I2',12X,'I3'//40X,'I0(I)',3(3X,F
  10.4)/40X,'P0(I)',3(3X,F10.4)/40X,'RT(I)',3(3X,F10.6)/40X,'R(I)
  21',3(3X,F10.6)/40X,'R0(I)',3(3X,F10.6)/42X,'VX0(I)',3(3X,F10.4)
  3/40X,'R(I)',3(3X,F10.5)/40X,'A0(I)',3(3X,F10.5)/40X,'A1(I)',3(
  43X,F10.5)/40X,'A2(I)',3(3X,F10.5)/)
215 FORMAT('I',14X,'THE FOLLOWING LINES ARE USEFUL FOR DEBUGGING')
218 FORMAT('O',14X,'ITERATION TERMINATED DUE TO DIVERGING VALUE OF DR
  1',20X,'I=',I4,3X,'I2=',I5,3X,'I3=',I5)
220 FORMAT(15X,'I1=',I4,3X,'I=',I3,3X,'I2=',I4,3X,'I3=',I4,3X,'I4',I4,3X,'I5',F10.
  1,5,3X,'DR=',F10.4,3X,'VXR(I)=',F12.6)
225 FORMAT('O',14X,'ITERATION TERMINATED DUE TO DIVERGING VALUE OF S')
231 FORMAT('I',41X,'RESULTS FOR SRE MODIFIED BY FLARE, DISK')
232 FORMAT('I',47X,'RESULTS FOR SRE, UNMODIFIED')
240 FORMAT('O',44X,'PLANE NO.',I2,4X,'VXR(I2,')=',F10.4/55X,'J',5X,'
  1R',10X,'U',9X,'VX',I2,7X,'VT',I2,9X,'V',I2,7X,'ALPHA',I2
  2,4X,'BETA',I2,5X,'MV',I2,6X,'MM',I2,/)

```



```

250 FORMAT(3X,I3,1X,F9.5,2X,F8.3,4(2X,F10.5),2X,2(F9.4,2X),2(F8.5,2X))
252 FORMAT('0',45X,'FF=',F10.6,3X,'DD=',F10.6,3X,'VXSPE=',F12.6)
260 FORMAT('0',35X,'J',6X,'V1/V2',7X,'W2/W1',6X,'DALPHA',5X,'DB-TA',/)
270 FORMAT(34X,I3,4(2X,F10.5))
411 FORMAT(33X,'L2=',I4,3X,'VVK=',F10.4,3X,'VX=',F10.4,3X,'DR=',F10.4
1,3X,'R(I,JJ)=' ,F10.6)
      END

```


B.2 Subroutine STREAM

STREAM calculates an $r_{i,j+1}$, iterating on assumed values for V_x and V_θ until $r_{i,j+1}$ and the average properties based on $r_{i,j}$ and $r_{i,j+1}$ are consistent.


```

SUBROUTINE STREAM(I)
C STREAM CALCULATES THE LOCATION OF THE NEXT STREAMLINE BY ITERATION
REAL R(3,11),VX(3,11),VT(3,11),VRATIO(11),VRATIO(11),DALPHA(11)
REAL DPFTA(11)
REAL MV,MW
COMMON A0(3),A1(3),A2(3),R(3),C1,ON, F(3,4),
1 GAMMA,C,HR,HS,IWRITE,IRFAD, J,JJ,JM1,K,L1,L2,L3,PI,P0(3),R0(3),
2 R,RR,RT(3),RPM,REF,RGAS, TP(3),TEST1,TEST2,TEST3,TEST4,VX,VT,
3 VXR(3),VXA(3),WE,WS,WR,VXZ,VTZ
4,FF(3,11),DD(3,11),VXSPE(3,11)
IF(L1.EQ.1)RR=0(I,J)+(RT(I)-R(I,1))/FLOAT(JM1)
IF(L1.GT.1)RR=R(I,J+1)
N3=0
DRZ=RT(I)
RGUESS=RR
VX(I,J+1)=FVX(I)
VX(I,J+1)=VX(I,J+1)*FLARE(J)
IF(L1.EQ.1)GO TO 304
VX(I,J+1)=VX(I,J+1)*DISK(I)
304 IF(VX(I,J+1).LT.1.)WRITE(IWRITE,300)L1,L2,L3,I,J
VT(I,J+1)=FVT(I)
305 VXZ=(VX(I,J+1)+VX(I,J))/2.
VTZ=(VT(I,J+1)+VT(I,J))/2.
DRZOLD=DRZ
K(I,J+1)=KNEXT(I)
RR=R(I,J+1)
VX(I,J+1)=FVX(I)
VT(I,J+1)=FVT(I)
L3=L3+1
VXSRE(I,J+1)=VX(I,J+1)
VX(I,J+1)=VX(I,J+1)*FLARE(I)
FF(I,J+1)=FLARF(I)
IF(L1.EQ.1)GO TO 310

```



```

DD(I,J+1)=DISK(I)
VX(I,J+1)=VX(I,J+1)*DISK(I)
IF(VX(I,J+1).LT.1.)WRITE(IWRITE,300)L1,L2,L3,I,J
310 DRZ=ABS(R(I,J+1))-RGUESS)
IF(DRZ.LE.TEST2)RETURN
RGUESS=R(I,J+1)
C CHECK FOR DIVERGENCE OF J+1 STREAMLINE POSITION
IF(DRZ.GE.DRZOLD)N3=N3+1
IF(N3.LT.3)GO TO 305
WRITE(IWRITE,302)I,J,L1,L2,L3
C IF I=5 IS RETURNED, THE MAIN PROGRAM WILL GO ON TO A NEW DATA SET
I=5
RETURN
300 FORMAT(20X,'L1=',I4,3X,'L2=',I4,3X,'L3=',I4,3X,'I=',I3,3X,'J=',I4,
125X,'VX(I,J) LESS THAN 1.0 FT/SEC')
302 FORMAT('0',I4X,'ITERATION TERMINATED DUE TO DIVERGING POSITION OF
1 STREAMLINE J+1',/,20X,'I=',I4,3X,'J=',I5,3X,'L1=',I4,3X,'L2=',I5,3
2X,'L3=',I5)
END

```


B.3 Function Subprograms

The listing for each of the five function subprograms appears on one of the following pages.

<u>Function</u>	<u>Page</u>	<u>Description</u>
RNEXT	107	given a value of $r_{i,j}$ and the properties V_x , V_θ , RNEXT calculates a trial $r_{i,j+1}$
FLARE	108	given $r_{i,j+1}$, FLARE calculates a non-dimensional factor which, multiplied by V_x in STREAM, gives a V_x modified for FLARE
DISK	109	given appropriate values of $V_{xi,j}$, DISK calculates a non-dimensional factor used to modify axial velocity for actuator disk effects
FVT	110	given $r_{i,j}$, FVT calculates a V_θ by a proposed simple quadratic relation
FVX	111	given $r_{i,j}$, FVX calculates a V_x using a simple radial equilibrium relation


```

FUNCTION RNEXT(I)
C RNEXT--CALCULATES A TRIAL LOCATION FOR THE NEXT STREAMLINE GIVEN THE AVERAGE
C VELOCITIES VX AND VT AND THE LOCATION OF THE CURRENT STREAMLINE
      REAL R(3,11),VX(3,11),VT(3,11),VRATIO(11),WRATIO(11),DALPHA(11)
      REAL DFETA(11)
      REAL MV,Ma
      COMMON AQ(3),A1(3),A2(3),B(3),C1,DN,      F(3,4),
      GAMMA,G,HP,HS,IWRITE,IREAD,  J,JJ,JM1,K,L1,L2,L3,PI,P0(3),R0(3),
      PR,RR,RT(3),RPM,REF,RGAS,      T0(3),TEST1,TEST2,TEST3,TEST4,VX,VT,
      VXE(3),VXZ(3),DE,WS,WR,VXZ,VTZ
      L,FF(3,11),DD(3,11),VXSRE(3,11)
      VV=VXZ*VXZ+VTZ*VTZ
      TR=1./C1*VV/T0(I)
      RHO=TR**(1./(GAMMA-1.))*P0(I)/RGAS/T0(I) *144.
      AREA=DN/RHO/VXZ
      RNEXT=SQRT(R(I,J)*R(I,J)+AREA/PI)
      RETURN
END

```



```

FUNCTION FLARE(I)
C FLARE--COMPUTES THE GEOMETRIC VX VELOCITY CORRECTION FACTOR DUE TO FLARE
REAL R(3,11),VX(3,11),VT(3,11),VRATIO(11),WRATIO(11),DALPHA(11)
REAL DPRETA(11)
REAL MV,MA
COMMON A0(3),A1(3),A2(3),R(3),C1,DM, F(3,4),
1 GAMMA,G,HX,HS,IMRITE,IRFAD, J,JJ,JM1,K,L1,L2,L3,PI,PC(3),Rn(3),
2 K,RR,RT(3),RPM,REF,PGAS, T0(3),TEST1,TEST2,TEST3,TEST4,VX,VT,
3 VXR(3),VXW(3),VE,WS,WR,VXZ,VIZ
4,FF(3,11),DD(3,11),VXSRE(3,11)
IF(I.LE.1)D=WE
IF(I.EQ.2)D=WE+WS
IF(I.GE.3)D=WE+WS+WP
TGNT=(PR-REF)/D
FLARE=1.0/(TGNT*TGNT+1.0)
RETURN
END

```



```

FUNCTION DISK(J)
C DISK--COMPUTES THE VX VELOCITY CORRECTION FACTOR PER ACTUATOR DISK THEORY
REAL R(3,11),VX(3,11),VT(3,11),VRATIO(11),VRATIO(11),DALPHA(11)
REAL DPETA(11)
REAL MV,MV
. COMMON A0(3),A1(3),A2(3),R(3),C1,DM, F(3,4),
1 GAMMA,C,HH,HS,IWRITE,IFFAD, J,JJ,JM1,K,L1,L2,L3,PI,P0(3),Rn(3),
2 R,RR,RT(3),RPM,REF,PGAS, T0(3),TEST1,TEST2,TEST3,TEST4,VX,VT,
3 VXR(3),VXA(3),VE,WS,WF,VXZ,VTZ
4,FF(3,11),FD(3,11),VXSFF(3,11)
1 IF(1,LF,1)DISK=1.0+(VX(2,J+1)-VX(1,J+1))*EXP(-PI*WS/(2.0*HS))/(2.0*X
2 VX(1,J+1))
1 IF(1,EC,2)DISK=1.0+(VX(3,J+1)-VX(2,J+1))*EXP(-PI*WR/(2.0*HR))/(2.0*X
2 VX(2,J+1))-(VX(2,J+1)-VX(1,J+1))*EXP(-PI*WS/(2.0*HS))/(2.0*VX(2,J+1)
3 )
1 IF(1,GE,3)DISK=1.0-(VX(3,J+1)-VX(2,J+1))*EXP(-PI*WR/(2.0*HR))/(2.0*X
2 VX(3,J+1))
1 RETURN
END

```



```

FUNCTION FVX(I)
C FVX- COMPUTES VX AS A SRE FUNCTION OF R
REAL R(3,11),VX(3,11),VT(3,11),VRATIO(11),RATIO(11),DALPHA(11)
REAL DRETA(11)
REAL MV,MW
COMMON A0(3),A1(3),A2(3),R(3),C1,DM, F(3,4),
1 GAMMA,G,HS,IWRITE,IREAD, J,JJ,JM1,K,L1,L2,L3,PI,P0(3),R0(3),
2 R,R,RT(3),RPM,REF,RGAS, T(3),TEST1,TEST2,TEST3,TEST4,VX,VT,
3 VXR(3),VXV(3),VE,WS,W, VXZ,VTZ
4 FF(3,11),DD(3,11),VXSOF(3,11)
Z1= -1.5*A2(I)*A2(I)*(R**4-R7(I)**4)
Z2= -10./9.*A1(I)*A2(I)*(R**3-R0(I)**3)
Z3= (-4.*A0(I)*A2(I)-2.*A1(I)*A1(I))*(R*R-R0(I)*R0(I))
Z4= -6.*(A2(I)*A1(I)+A2(I)*R(I))*(R-R0(I))
Z5= -(2.*A0(I)*A2(I)+4.*A1(I)*R(I))*ALOG(R/R0(I))
Z6=2.*A0(I)*R(I)*(1./R-1./R0(I))
Z=VXR(I)*VXR(I)+Z1+Z2+Z3+Z4+Z5+Z6
IF(Z.LE.0.)GO TO 400
FVX= SORT(Z)
RETURN
400 WRITE(IWRITE,410)L1,L2,L3,I,J
FVX=0.0
410 FORMAT(20X,'L1=',I4,'I4,3X','L2=',I4,'I4,3X','I=',I4,
125X,'SORT ARGUMENT NEGATIVE')
RETURN
END

```



```

FUNCTION FVT(I)
C FVT=COMPUTES VT AS A FUNCTION OF R
      REAL R(3,11),VX(3,11),VT(3,11),VRATIO(11),WRATIO(11),DALPHA(11)
      REAL DBETA(11)
      REAL MV,MW
      COMMON A0(3),A1(3),A2(3),R(3),C1,DM,      F(3,4),
      IGAMMA,G,HR,HS,IWRITE,IREAD,  J,JJ,JM1,K,L1,L2,L3,PI,P0(3),RA(3),
      PR,RR,RT(3),RPM,REF,RGAS,      T0(3),TEST1,TEST2,TEST3,TEST4,VX,VT,
      VXR(3),VX2(3),VE,WS,WR,VXZ,VTZ
      A,FF(3,11),DD(3,11),VXSRE(3,11)
      FVT= A2(I)*RR*RR+A1(I)*RR+AC(I)+R(I)/RR
      RETURN
END

```


APPENDIX C

Specific Instructions For Use of the Program

C.1 General

This appendix is intended to provide detailed instructions for the use of the computer program developed in this thesis. Preparation of the input deck and interpretation of the output will be covered.

The program was run on the Interdata 70 computer at the Joint Mechanical and Civil Engineering Computer Facility at MIT, but should be easily adaptable to any FORTRAN IV capable system. References 7 and 8 served as the FORTRAN IV language guide. All READ and WRITE instructions are written with dummy variables IREAD and IWRITE, respectively. Therefore, the only two FORTRAN statements which need to be changed in order to run on another system using different input/output channel numbers are the two assigning integer values to IREAD and IWRITE. The control cards, listed below, which may be system dependent, are marked by an asterisk.

C.2 Loading Sequence

Listed below, in the sequence that they should be loaded, are the constituents of the program:

- * (1) Job card
- * (2) Language and other compilation control cards

- (3) MAIN program
- (4) Subprograms (in any order)
 - a) subroutine STREAM
 - b) function subprogram RNEXT
 - c) function subprogram FLARE
 - d) function subprogram DISK
 - e) function subprogram FVT
 - f) function subprogram FVX
- *(5) Execute card
- *(6) Common length designation and the execution control cards
- (7) Data cards
- *(8) Job termination card

C.3 Job Control Cards*

The program segments marked by an asterisk may vary in content and format from system to system or with time, and must be determined from an appropriate user's manual. It should be noted that the amount of blank common utilized by the program depends upon the dimension of some of the variables, which relates to the number of streamlines considered.

C.4 Data Cards

The data deck is composed of any number of separate data sets stacked directly together. Each set is independent of every other set and represents a separate simple radial equilibrium turbine design to be processed by the program.

Each data set consists of ten separate cards which must be present and in the proper sequence. A specific format is given for the data on each card, although free format (data fields separated by commas) may be used if the computer system has that feature.

The context of each card is given below in paragraph C.4.1. A superscript refers to an explanatory note in paragraph C.4.2.

C.4.1 Format Table

<u>Columns</u>	<u>Format</u>	<u>Information</u>	<u>Units</u>
<u>CARD ONE</u>			
1-4	I4	number of streamlines ¹	none
5-8	I4	diagnostics print key ²	none
9-12	I4	user data set number ³	none
<u>CARD TWO</u>			
1-10	F10.4	gamma (ratio of specific heats)	none
11-20	F10.4	specific gas constant	ft lbf/lbm/°R
<u>CARD THREE</u>			
1-9	F9.3	turbine rpm	rpm
10-18	F9.3	total mass flow rate	lbm/sec
19-27	F9.3	total temperature, plane 1	°R
28-36	F9.3	total pressure, plane 1	psi
37-45	F9.3	total temperature, plane 2	°R
46-54	F9.3	total pressure, plane 2	psi
55-63	F9.3	total temperature, plane 3	°R
64-72	F9.3	total pressure, plane 3	psi

CARD FOUR

1-10	F10.6	hub radius, plane 1	ft
11-20	F10.6	tip radius, plane 1	ft
21-30	F10.6	hub radius, plane 3	ft
31-40	F10.6	tip radius, plane 3	ft
41-50	F10.6	stator width	ft
51-60	F10.6	rotor width	ft

CARD FIVE

1-10	F10.6	test percent 1 ⁴	none
11-20	F10.6	test percent 2	none
21-30	F10.6	test percent 3	none
31-40	F10.6	test value 4	ft

CARD SIX

1-10	F10.6	SRE reference radius, plane 1	ft
11-20	F10.6	SRE reference velocity, plane 1	ft/sec
21-30	F10.6	SRE reference radius, plane 2	ft
31-40	F10.6	SRE reference velocity, plane 2	ft/sec
41-50	F10.6	SRE reference radius, plane 3	ft
51-60	F10.6	SRE reference velocity, plane 3	ft/sec

CARD SEVEN

1-10	F10.5	B for plane 1 ⁵	ft ² /sec
11-20	F10.5	A ₀ for plane 1	ft/sec
21-30	F10.5	A ₁ for plane 1	sec ⁻¹
31-40	F10.5	A ₂ for plane 1	ft ⁻¹ sec ⁻¹

CARD EIGHT

(Same as card seven, but for plane 2)

CARD NINE

(Same as card seven, but for plane 3)

CARD TEN

(The tenth card is blank)

C.4.2 Notes

1. The limit on the number of streamlines is only a practical one, related to machine computing speed and storage, and can be any reasonable number. The program was originally run with eleven; any greater number will require a new DIMENSION statement for the main and all subprograms. Additional blank common space may also have to be allocated.

2. If this data bit=1, all available diagnostics will be printed out. See paragraph C.5.3, below. If not equal to unity, no diagnostics except error messages will be printed out.

3. The user may use any three digit number to identify particular data sets. Some number must be supplied.

4. Refer to paragraph 3.3.13.

5. B , A_0 , A_1 , A_2 , are the coefficients of powers of r in the tangential velocity relation. See paragraph 3.3.6.

C.5 Output Discription

C.5.1 General

The output for each data set may be considered in three parts:

- (1) introductory
- (2) diagnostic (optional)
- (3) velocity triangle data
 - (i) modified simple radial equilibrium values
 - (ii) SRE values.

C.5.2 Introductory Output

Input data and other selected calculated values, which do not change during the execution of a data set, are printed out in the introductory block. The symbols appearing have the same meaning as used in the program and given in Appendix A. If the data is input also, the output units are the same. TEST1, TEST2, TEST3, REF, and WE have units of feet, and PHITIP and PHIHUB are in degrees.

C.5.3 Diagnostic Output

If input variable KK=1, certain lines of information are printed out during execution of the program iterations. Sample output of this type is shown at the end of this appendix. Each line contains the current values of certain important variables of the program at a certain step in the calculations. This information was used in the development of the program and should not be

required routinely. However, it can increase confidence in the results, and may be useful if unexpected problems occur during operation in the future. Additional details on the meaning of the loop counters can be learned from the flow charts presented in Chapter 3.

C.5.4 Velocity Triangle Output

A group of results is printed for each of two cases:

(1) The streamline numbers and locations, and velocity results are printed for a simple radial equilibrium preliminary design which has been modified by the flare and actuator disk corrections determined by the program. Results pertaining to each of the planes is printed, followed by a block of results involving values from more than one plane.

(2) For comparison purposes, values calculated at the same streamlines as above, but with no modification for flare and actuator disk are printed in the same format.

The meanings of the variables are the same as listed in Appendix A, or are self-explanatory. The 1 and 2 appearing in some column labels refer to rotor inlet and outlet triangle, respectively, following the usual convention. Distances are in feet, velocities in ft/sec, and angles in degrees. The value $VXR(I)$ printed for each plane is the final value for the constant term in the FVX relation for axial velocity. It was changed from $VX\emptyset(I)$ to satisfy continuity.

C.5.5 Error Messages

The input data to this program is assumed to be from a feasible preliminary design. Therefore, many types of execution errors, such as from the appearance of negative radii, should not occur. If some inconsistent or infeasible data should be used, however, measures have been taken to minimize the chances of hanging the program up in an iteration loop. The details of the testing procedure to accomplish this are found in paragraph 3.4. Each iterative loop is provided with a means of exit if the error term increases for at least two successive iterations. Another check is made to determine if the axial velocity is less than 1.0 ft/sec (an arbitrary, small positive value, to avoid the possibility of dividing by zero).

If any of the conditions listed in the next paragraph are discovered, an error message will be printed out regardless of whether or not the user has specified the printing of the diagnostic data.

The following is a list of error conditions tested for, and their corresponding output messages:

- (1) Condition: the axial velocity computed by the function subprogram FVX is less than 1.0 ft/sec

Error message: L1 = xxx L2 = xxx L3 = xxx
I = xxx J = xxx VX(I,J) LESS
THAN 1.0 FT/SEC

Action: execution continues

- (2) Condition: the change, S , in the $I=3$ plane
streamline positions is not
decreasing on successive iterations

Error message: ITERATION TERMINATED DUE TO
INCREASING VALUES OF S

Action: execution of current data set is
terminated

- (3) Condition: the annulus geometry error, DR ,
is not decreasing on successive
iterations

Error message: ITERATION TERMINATED DUE TO
INCREASING VALUES OF DR

$I = \text{xxx}$ $L2 = \text{xxx}$ $L3 = \text{xxx}$

Action: execution of current data set is
terminated

- (4) Condition: the change, DRZ , in the calculation
of $R(I,J+1)$ by subroutine STREAM
is not decreasing on successive
iterations

Error message: ITERATION TERMINATED DUE TO
DIVERGING POSITION OF STREAM-

LINE $J+1$ $I = \text{xxx}$ $J = \text{xxx}$

$L1 = \text{xxx}$ $L2 = \text{xxx}$ $L3 = \text{xxx}$

Action: execution of current data set is
terminated

C.6 Additional Options

In some applications it may be desired to find the simple radial equilibrium streamlines, or to consider the effects of the flare or actuator disk correction alone. To accomplish this, the executable statements in one or both of the subprograms FLARE(I) and DISK(I) may be replaced by the statement FLARE = 1.0 or DISK = 1.0, as appropriate.

TYPE FOLLOWING LINES ARE USEFUL FOR DEBUGGING									
L2=	1	VBP=	164,0200	VX=	01,2690	DB=	4,0047	R(1,0)=	1,142,72
L2=	2	VBP=	190,6020	VX=	131,1155	DB=	-4,00470	R(1,0)=	1,114,40
L2=	3	VBP=	191,0854	VX=	121,6569	DB=	4,00474	R(1,0)=	1,126,20
L2=	4	L2=	82 S=	0,2137	DB=	-4,0007	VX=11=	193,8373-1	
L2=	1	VBP=	164,0400	VX=	04,03135	DB=	0,0577	R(1,0)=	1,124,74
L2=	2	VBP=	201,7891	VX=	130,5375	DB=	-4,00494	R(1,0)=	1,170,175
L2=	3	L2=	61 S=	0,2764	DB=	0,2005	VX=11=	190,827612	
L2=	1	VBP=	164,0400	VX=	01,7462	DB=	4,0535	R(1,0)=	1,130,48
L2=	2	VBP=	190,4087	VX=	120,3312	DB=	-4,00471	R(1,0)=	1,127,03
L2=	3	VBP=	193,0674	VX=	123,4495	DB=	4,00418	R(1,0)=	1,124,700
L2=	4	L2=	85 S=	0,2765	DB=	-4,0004	VX=11=	190,281264	
L2=	1	VBP=	193,8373	VX=	125,8179	DB=	-4,0017	R(1,0)=	1,110,115
L2=	2	L2=	76 S=	0,00724	DB=	-4,0002	VX=11=	191,856964	
L2=	1	VBP=	194,0276	VX=	125,4485	DB=	4,0033	R(1,0)=	1,140,40
L2=	2	VBP=	201,6723	VX=	126,2583	DB=	4,00419	R(1,0)=	1,140,62
L2=	3	L2=	56 S=	0,00390	DB=	0,0012	VX=11=	192,376345	
L2=	1	VBP=	194,3813	VX=	125,7478	DB=	-1,0019	R(1,0)=	1,124,140
L2=	2	L2=	30 S=	0,00732	DB=	-4,0004	VX=11=	192,01,381	
L2=	1	L2=	12 S=	0,00104	DB=	-4,0001	VX=11=	191,856964	
L2=	2	L2=	16 S=	0,00032	DB=	-4,0012	VX=11=	193,37635-	
L2=	1	L2=	1 S=	0,00005	DB=	-4,0004	VX=11=	193,83,381	

Figure C-1

APPENDIX D

Integration of the Simple Radial Equilibrium Equation

A convenient form of the simple radial equilibrium equation is

$$-V_x \frac{dV_x}{dr} = \frac{V_\theta}{r} \frac{d}{dr}(rV_\theta). \quad (D.1)$$

Given explicit functions, $V_\theta(r)$, it can be easily integrated to find a relation for axial velocity as a function of radius.

Suppose the expression for the tangential velocity, $V_\theta(r)$, can be written in the following form:

$$V_\theta(r) = a_2 r^2 + a_1 r + a_0 \mp \frac{b}{r}. \quad (D.2)$$

The bottom sign applies after a stator row, and the top sign applies after a rotor row.

Then, proceeding to evaluate the right hand side of equation (D.1),

$$rV_\theta = a_2 r^3 + a_1 r^2 + a_0 r \mp b$$

$$\frac{d}{dr}(rV_\theta) = 3a_2 r^2 + 2a_1 r + a_0$$

$$\frac{1}{r} \frac{d}{dr}(rV_\theta) = 3a_2 r + 2a_1 + \frac{a_0}{r}; \quad (D.3)$$

Finally, multiplying (D.2) by (D.3), (D.1) becomes

$$\begin{aligned}
 -V_x \frac{dV_x}{dr} = & 3a_2^2 r^3 + 5a_1 a_2 r^2 + (4a_o a_2 + 2a_1^2) r \\
 & + (3a_o a_1 + 3a_2 b) + (a_o^2 + 2a_1 b) \frac{1}{r} + \frac{a_o b}{r^2} \quad (D.4)
 \end{aligned}$$

Equation (D.4) may be integrated directly from a reference radius, r_i , and axial velocity, V_{xi} , to an arbitrary radius r , and corresponding V_x . This gives

$$\begin{aligned}
 -\frac{1}{2}(V_x^2 - V_{xi}^2) = & \frac{3}{4}a_2^2(r^4 - r_i^4) + \frac{5}{3}a_1 a_2(r^3 - r_i^3) \\
 & + (2a_o a_2 + a_1^2)(r^2 - r_i^2) + 3(a_o a_1 + a_2 b)(r - r_i) \\
 & + (a_o^2 + 2a_1 b) \ln\left(\frac{r}{r_i}\right) + a_o b \left(\frac{1}{r} - \frac{1}{r_i}\right).
 \end{aligned}$$

Rearranging,

$$\begin{aligned}
 V_x^2 - V_{xi}^2 = & -\frac{3}{2}a_2^2(r^4 - r_i^4) - \frac{10}{3}a_1 a_2(r^3 - r_i^3) \\
 & - (4a_o a_2 + 2a_1^2)(r^2 - r_i^2) - 6(a_o a_1 + a_2 b)(r - r_i) \\
 & - (2a_o^2 + 4a_1 b) \ln(r/r_i) + 2a_o b \left(\frac{1}{r} - \frac{1}{r_i}\right). \quad (D.5)
 \end{aligned}$$

The general expression, (D.5), may be simplified for two special cases in common use:

(i) Let $a_2 = a_o = 0$; $a_1, b \neq 0$. Then (D.5) becomes

$$V_x^2 - V_{xi}^2 = -2a_1^2(r^2 - r_i^2) \pm 4a_1b \ln(r/r_i). \quad (D.6)$$

This represents the constant reaction type design.⁶

(ii) Let $a_2 = a_1 = 0$; $a_o, b \neq 0$. Then (D.5) becomes

$$V_x^2 - V_{xi}^2 = -2a_o^2 \ln(r/r_i) \mp 2a_ob\left(\frac{1}{r} - \frac{1}{r_i}\right). \quad (D.7)$$

This represents a design in which the stator inlet angle, α_2 , is approximately the same at all radii.⁶

APPENDIX E

Actuator Disk Superposition

Approximate solutions of the actuator disk theory, discussed in Chapter 2, are, in the case of the isolated disk:

$$V_x = (V_x)_{-\infty} + \frac{(V_x)_{+\infty} - (V_x)_{-\infty}}{2} \exp\left(\frac{\pi x}{h}\right), \quad (\text{E.1})$$

upstream of the disk ($x < 0$), and

$$V_x = (V_x)_{+\infty} - \frac{(V_x)_{+\infty} - (V_x)_{-\infty}}{2} \exp\left(-\frac{\pi x}{h}\right) \quad (\text{E.2})$$

downstream of the disk ($x > 0$).

These equations pertain to the axial variation of axial velocity along a streamline.

Suppose it is desired to consider the effects of these actuator disk solutions at the three principal planes of a single stage axial turbine. Two actuator disks are involved, corresponding to the stator row and the rotor row. The three planes of interest are the stator leading edge (plane 1), the rotor leading edge (plane 2), and the rotor trailing edge (plane 3).

For simplicity, assume that the stator leading edge is influenced only by the stator actuator disk (for equal blade widths, the rotor disk is three times

the distance away), and that the rotor trailing edge is influenced only by the rotor actuator disk. The rotor leading edge feels the effects of both the stator and rotor disks. Refer to Figure E-1.

The relations (E.1) and (E.2) apply to the stage inlet and outlet planes respectively. The effect at the rotor leading edge, point S, can be obtained by superimposing the velocity corrections due to the two disks. The effect of the stator upon S is given by (E.1) with $x = -WS/2$ and $h = HS$; the effect of the rotor is given by (E.2) with $x = +WR/2$ and $h = HR$.

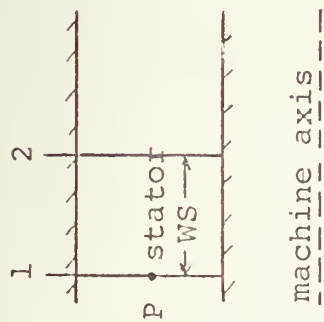
In addition, the velocities at infinity, appearing in the two equations must be interpreted. Let $(V_{xr})_{+\infty}$ denote the axial velocity a long way downstream of the rotor disk; similarly, let $(V_{xs})_{-\infty}$ denote the axial velocity a long way upstream from the stator, and so on. Then (E.1) and (E.2) become

$$V_x = (V_{xr})_{-\infty} + \frac{(V_{xr})_{+\infty} - (V_{xr})_{-\infty}}{2} \exp\left(-\frac{\pi \cdot WR}{2 \cdot HB}\right), \quad (E.3)$$

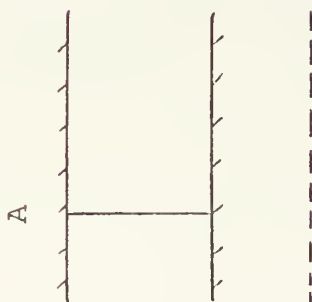
which is the effect of the rotor, and

$$V_x = (V_{xs})_{+\infty} - \frac{(V_{xs})_{+\infty} - (V_{xs})_{-\infty}}{2} \exp\left(-\frac{\pi \cdot WS}{2 \cdot HS}\right), \quad (E.4)$$

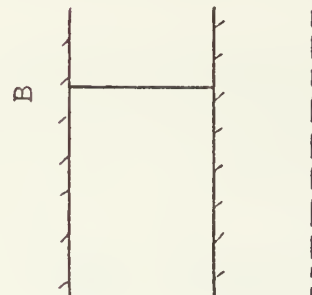
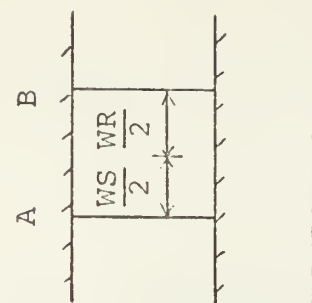
which is the effect of the stator upon point S.



Turbine
Blading

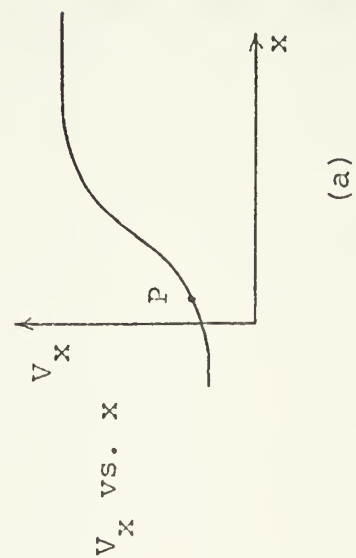


Actuator
Disks

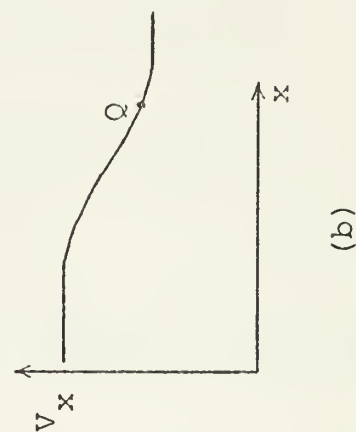


A B

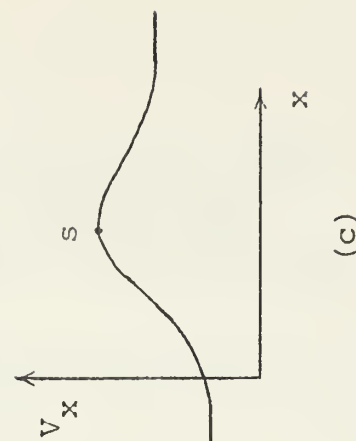
$$\frac{WS}{2} \quad \frac{WR}{2}$$



(a)



(b)



(c)

Figure E-1

Now assume

$$(V_{xr})_{-\infty} = (V_{xs})_{+\infty} = V_{xm} = \text{the simple radial equilibrium velocity at the rotor leading edge (plane 2) corrected for flare;}$$

$$(V_{xs})_{-\infty} = V_{x-} = \text{the axial velocity at plane 1;}$$

$$(V_{xr})_{+\infty} = V_{x+} = \text{the axial velocity at plane 3.}$$

Then finally, the corrected axial velocity, V_{x2} , at point S (plane 2) can be written

$$\frac{V_{x2}}{V_{xm}} = 1 + \frac{V_{x+} - V_{xm}}{2V_{xm}} \exp\left(-\frac{\pi \cdot WR}{2 \cdot HR}\right) - \frac{V_{xm} - V_{x-}}{2V_{xm}} \exp\left(-\frac{\pi \cdot WS}{2 \cdot HS}\right).$$

(E.5)

V_{x2} is the axial velocity corrected for both flare and actuator disk effects.

APPENDIX F

Calculation of the Flare Geometry Factors

The purpose of this appendix is to derive the two parameters REF and WE used by the computer program to compute the flare angle ϕ . The computation of ϕ at an arbitrary point, Q, within the annulus is also demonstrated. The stage inlet and outlet hub and shroud radii are given information.

Referring to Figure F-1, on the next page, it is seen that the point P is the intersection of the extended line segments forming the hub and shroud walls of the turbine. The line $x = 0$ represents the inlet plane of the turbine, $x = x_3$ represents the outlet plane, and $y = 0$ represents the axis of the machine.

The equations for the lines representing the shroud and hub walls, respectively, are written as

$$y = \frac{(R_{t3} - R_{t1})}{x_3} x + R_{t1} \quad (F.1)$$

$$y = \frac{(R_{h3} - R_{h1})}{x_3} x + R_{h1}. \quad (F.2)$$

Solving (F.1) and (F.2) simultaneously for x and y , the coordinates of the point P, namely $(-WE, REF)$, are found to be

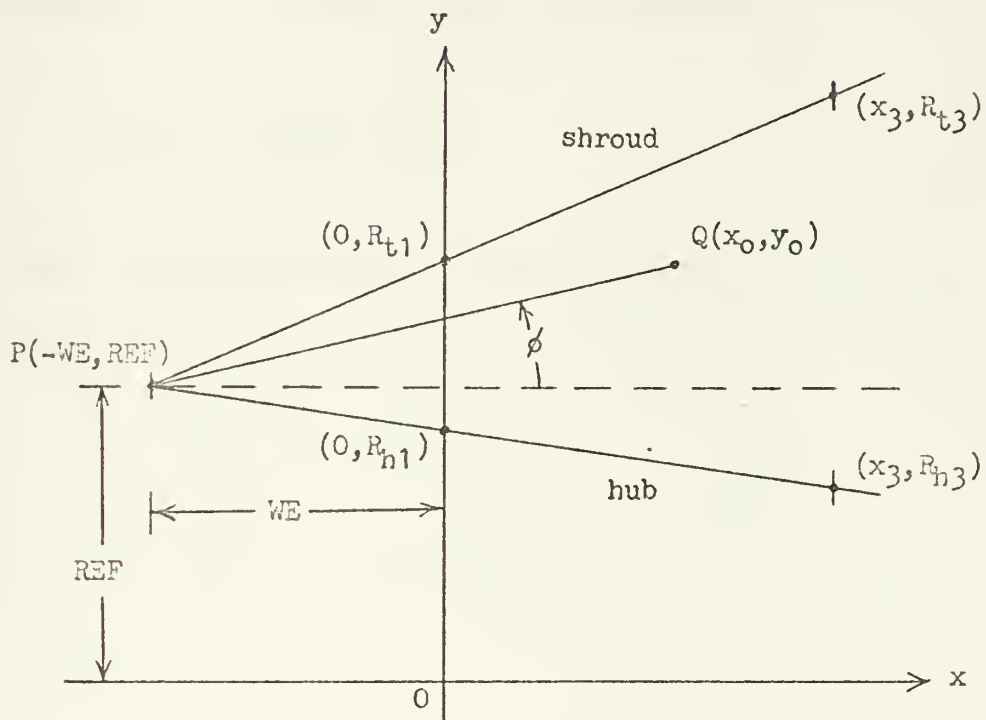


Figure F-1

$$WE = \frac{(R_{t1} - R_{h1})x_3}{R_{t3} - R_{t1} - R_{h3} + R_{h1}} , \quad (WE > 0) \quad (F.3)$$

$$REF = R_{h1} + \frac{WE}{x_3} (R_{h1} - R_{h3}) . \quad (F.4)$$

The angle ϕ for some arbitrary point, Q, within the annulus, can be found from the expression

$$\tan \phi = \frac{y_o - REF}{WE + x_o} , \quad (F.5)$$

where the coordinates of the point Q are (x_o, y_o) .

Thesis

103423

L2745 Larson

Improvements to simple radial equilibrium preliminary turbine design.

17 FEB 76
1 FEB 76

DISPLAY
DISPLAY

Thesis

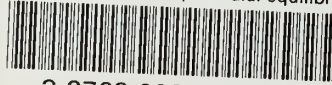
103428

L2745 Larson

Improvements to simple radial equilibrium preliminary turbine design.

thesL2745

Improvements to simple radial equilibriu



3 2768 002 12270 7

DUDLEY KNOX LIBRARY